

Impacts of Land-Use and Biofuels Policy on Climate: Temperature and Localized Impacts

Willow Hallgren, Adam Schlosser and Erwan Monier



Report No. 227
August 2012

The MIT Joint Program on the Science and Policy of Global Change is an organization for research, independent policy analysis, and public education in global environmental change. It seeks to provide leadership in understanding scientific, economic, and ecological aspects of this difficult issue, and combining them into policy assessments that serve the needs of ongoing national and international discussions. To this end, the Program brings together an interdisciplinary group from two established research centers at MIT: the Center for Global Change Science (CGCS) and the Center for Energy and Environmental Policy Research (CEEPR). These two centers bridge many key areas of the needed intellectual work, and additional essential areas are covered by other MIT departments, by collaboration with the Ecosystems Center of the Marine Biology Laboratory (MBL) at Woods Hole, and by short- and long-term visitors to the Program. The Program involves sponsorship and active participation by industry, government, and non-profit organizations.

To inform processes of policy development and implementation, climate change research needs to focus on improving the prediction of those variables that are most relevant to economic, social, and environmental effects. In turn, the greenhouse gas and atmospheric aerosol assumptions underlying climate analysis need to be related to the economic, technological, and political forces that drive emissions, and to the results of international agreements and mitigation. Further, assessments of possible societal and ecosystem impacts, and analysis of mitigation strategies, need to be based on realistic evaluation of the uncertainties of climate science.

This report is one of a series intended to communicate research results and improve public understanding of climate issues, thereby contributing to informed debate about the climate issue, the uncertainties, and the economic and social implications of policy alternatives. Titles in the Report Series to date are listed on the inside back cover.

Ronald G. Prinn and John M. Reilly
Program Co-Directors

For more information, please contact the Joint Program Office

Postal Address: Joint Program on the Science and Policy of Global Change
77 Massachusetts Avenue
MIT E19-411
Cambridge MA 02139-4307 (USA)
Location: 400 Main Street, Cambridge
Building E19, Room 411
Massachusetts Institute of Technology
Access: Phone: +1.617. 253.7492
Fax: +1.617.253.9845
E-mail: globalchange@mit.edu
Web site: <http://globalchange.mit.edu/>

 Printed on recycled paper

Impacts of Land-Use and Biofuels Policy on Climate: Temperature and Localized Impacts

Willow Hallgren*[†], Adam Schlosser* and Erwan Monier*

Abstract

The impact on climate of future land-use and energy policy scenarios is explored using two land-use frameworks: (i) Pure Cost Conversion Response (PCCR), or 'extensification', where the price of land is the only constraint to convert land to agricultural production, including growing biofuels, and (ii) Observed Land Supply Response (OLSR), or 'intensification', where legal, environmental and other constraints encourage more intense use of existing managed land. These two land-use frameworks, involving different economic assumptions, were used to explore how the large-scale plantation of cellulosic biofuels to meet global energy demand impacts the future climate. The land cover of the Community Atmospheric Model Version 3.0 (CAM3.0) was manipulated to reflect these two different land-use and energy scenarios (i.e. biofuels and no biofuels). Using these landscapes, present and future climate conditions were simulated to assess the land cover impact. In both the intensification and extensification scenarios, the biofuel energy policy increases the land reflectivity of many areas of the globe, indicating that biofuel cropland is replacing darker land-vegetation, which directly leads to cooling. Moreover, the extensification framework—which involves more deforestation than the intensification framework—leads to larger increases in the reflectivity of the Earth's surface and thus a stronger cooling of the land surface in the extratropics. However, the deforestation which occurred in the tropics produced an increase in temperature due to a decrease in evaporative cooling and cloud cover, and an increase in insolation and sensible heating of the near surface. Nevertheless, these surface-air temperature changes associated with land-use are smaller than the effect from changes in the trace-gas forcing (i.e. the enhanced greenhouse effect), although over some regions the land-use change can be large enough to counteract the human-induced, radiatively forced warming. A comparison of these biogeophysical impacts on climate of the land-use and biofuel policies with the previously published biogeochemical impact of biofuels indicates the dominance of biogeophysical impacts at 2050.

Contents

1. INTRODUCTION.....	2
2. METHODS.....	3
2.1 Models Used.....	3
2.1.1. Community Atmosphere Model (CAM 3.1).....	3
2.1.2. Community Land Model (CLM3.0).....	4
2.2 Data Used.....	5
2.3 Modification of the Land Surface in CLM.....	5
2.4. Modeling Scenarios.....	7
2.4.1. Pure Conversion Cost Response Model (PCCR).....	7
2.4.2. Observed Land Supply Response Model (OLSR).....	9
2.5. Experimental Design.....	9
3. RESULTS AND DISCUSSION.....	11
3.1 IGSM-TEM Land Cover Change from 1990 to 2050: 4 Scenarios.....	12
3.2. The Impacts of Different Land-Use and Biofuels Policies on the Surface	
Climate.....	12
3.2.1. Albedo, Net Radiation and the Surface Energy Balance.....	13
3.2.2. Temperature: The Integrated Response.....	26

* Joint Program on the Science and Policy of Global Change, MIT, Cambridge, MA, USA

[†] Corresponding Author: Willow Hallgren (Email: hallgren@mit.edu)

3.3 A Preliminary Comparison of the Biogeophysical and Biogeochemical Impacts of the Biofuel Policy.....	32
4. CLOSING REMARKS.....	34
5. REFERENCES.....	36
APPENDIX.....	39

1. INTRODUCTION

Economic studies estimate that future global energy demands will increase from the about 400 exajoules of world commercial energy consumption at the end of the 20th century—15% of which is from non-fossil fuel sources—to between 550 and 1000 exajoules per year in 2050, depending on the availability of resources, and how policies to limit greenhouse gases affect energy demands in the future (Clarke *et al.*, 2007; Melillo *et al.*, 2009a). To meet these future energy demands, biofuels have been proposed as a potential low-carbon energy source that, along with other technologies (nuclear, hydro, wind, solar), will also reduce greenhouse gas emissions and provide some mitigation to global warming (Pacala and Socolow, 2004; Farrell *et al.*, 2006). Such alternate energy technologies would need to be implemented at very large scales, and although there has been some investigation into the climate impact on large scale wind farm installations (Wang and Prinn, 2010), apart from the impact on carbon emissions, there has been little research into the environmental impact of large scale biofuels plantation, with biofuel impact studies so far limited to small (local or sub-regional) scales (Searchinger *et al.*, 2008; Tilman *et al.*, 2006; Fargione *et al.*, 2008; Scharlemann and Laurance, 2008; The Royal Society, 2008).

However, there is good reason to suspect that such large-scale biofuel plantations will likely have a large impact on the Earth’s land surface, including the possibility of large areas of deforestation to make way for biofuels. There are many studies investigating the climate impact of land-use change, and also specifically deforestation (e.g., Pitman *et al.*, 2009; Bonan *et al.*, 2008; Henderson-Sellers *et al.*, 1993; Lee *et al.*, 2011). The evidence showing how deforestation can impact regional climate, with potential, and even likely, teleconnections, would suggest the need for a study which investigates the direct climatic impact of extensive land cover change due to future large scale planting of biofuels, in the context of changes in climate which are projected to occur in the period when the biofuel policy is being implemented. However, the use of biofuels to supply growing energy demands occurs in a complex context of economic factors (such as food prices, land prices etc.), population growth, environmental regulation, etc., which ideally should be taken into account when projecting where and how much biofuel crops are planted.

Melillo *et al.* (2009a) used a computable general equilibrium (CGE) model of the world economy, the MIT Emissions Predictions and Policy Analysis (EPPA) model (Paltsev *et al.*, 2005; Gurgel *et al.*, 2007), coupled with a process-based terrestrial biogeochemistry model, the Terrestrial Ecosystem Model (TEM) (Melillo *et al.*, 1993; Felzer *et al.*, 2004; Sokolov *et al.*, 2008), to generate two real-world global land-use scenarios in which an ambitious global cellulosic biofuels program over the first half of the 21st century was implemented to help meet

future energy demand. The biofuels scenarios were modeled within the framework of a global climate policy to control greenhouse gas emissions from industrial and fossil fuel sources, with the goal of stabilizing atmosphere's CO₂ concentration at 550 ppmv, not taking into account the feedbacks from land-use change (Paltsev *et al.*, 2008), which will be addressed in future research. The climate policy makes fossil fuel use more expensive and expedites the introduction of biofuels, increasing the size of the industry. The two land-use scenarios differed in terms of the economic frameworks, in which there were different constraints on the land supply which favored either deforestation or intensification of agricultural activities, in order to supply land to grow biofuels, as will be described in more detail below.

Melillo *et al.* (2009b) investigated the biogeochemical impact of these biofuel and land-use policies on the carbon balance, as well as the impacts on biodiversity, and the human footprint of the two land-use scenarios. This study builds on their analytical framework and sets out to investigate the climatic impact of a global cellulosic biofuels program up to 2050, in both of these economic scenarios, in the context of a changing climate. We address multiple questions of whether the policy of using biofuels to meet future energy needs has a statistically significant impact on a variety of local and non-local measures of climate, and compare this to the case where the biofuels policy is not implemented. We explore whether the economic framework used (and hence the presence or lack of environmental constraints on land-use) has a statistically significant impact on future climate; and how much of the total climate change seen in 2050 is solely due to land cover change, and how much is solely due to radiative forcing. We also compare the biogeophysical impact of biofuels production, as indicated by the temperature response resulting from the land-use changes implemented in our study, to the biogeochemical impact of biofuels, shown by Melillo *et al.* (2009b).

2. METHODS

2.1 Models Used

In this study, scenarios of land-use and cover (e.g., areas of cropland, tropical forests, etc.) are generated to reflect different economic frameworks and biofuel policy in 2050 by the coupling of an economics and ecological model within an integrated climate impact assessment framework (IGSM version 2.2) (Prinn *et al.*, 1999; Sokolov *et al.*, 2005). Areas of biofuel production were derived from the coupled economics-earth system-ecosystem model (**Figure 1**; stippled area), and fed into a coupled global climate-land surface-slab ocean model (Figure 1; non-stippled area), in order to simulate the impact on the global climate. These models are described in more detail below.

2.1.1. Community Atmosphere Model (CAM 3.1)

The National Center for Atmospheric Research (NCAR) Community Atmosphere Model (CAM 3.1) is the fifth generation of the NCAR atmospheric GCM (Collins *et al.*, 2004). This global climate model incorporates the NCAR Community Land Model (CLM), Version 3.0 (Oleson *et al.*, 2004), which is a Land Surface Model run as a component model within CAM. In

this study, CAM is also run with a slab ocean model in order to be able to generate some of the non-local feedbacks resulting from land cover change. The coupled CAM-CLM was run at a $2^\circ \times 2.5^\circ$ resolution in this study.

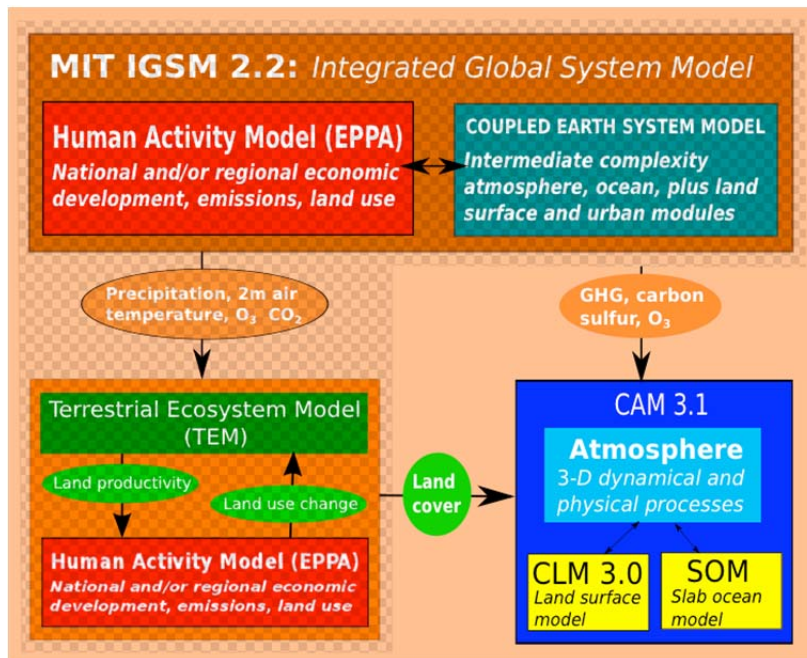


Figure 1. The offline coupling of IGSM 2.2 and CAM3.1-CLM3.0 used in this study. The stippling indicates the modeling framework used in Melillo *et al.* (2009).

CAM3.1 was first used in this study to generate initial states for both the atmosphere and land surface using output from a 20 year data-only model run (using fixed sea surface temperatures) for both the years 1990 and 2050. Then, two initialized equilibrium runs of 80 years each were done, using a simple, but interactive slab ocean model; the output was verified to have reached equilibrium, and the last 50 years of model output from both simulations was used for analysis.

2.1.2. Community Land Model (CLM3.0)

The NCAR Community Land Model, Version 3.0 is the land surface model used with CAM3.0 and the Community Climate System Model (CCSM3.0) (Vertenstein *et al.*, 2004). It is an improved, expanded version of its predecessor, the NCAR Land Surface Model (NCAR LSM), a community-developed land model focusing on biogeophysics, and now includes the carbon cycle, vegetation dynamics, and river routing (Oleson *et al.*, 2004).

The CLM is designed for coupling to atmospheric numerical models. It provides surface albedos (direct beam and diffuse for visible and near-infrared wavebands), upward longwave radiation, sensible heat flux, latent heat flux, water vapor flux, and zonal and meridional surface stresses required by atmospheric models. These are regulated in part by many ecological and hydrological processes, and the model simulates processes such as leaf phenology, stomatal physiology, and the hydrologic cycle. The model accounts for ecological differences among

vegetation types, hydraulic and thermal differences among soil types, and allows for multiple land cover types within a grid cell (Oleson *et al.*, 2004). Spatial land surface heterogeneity in CLM is represented as a nested subgrid hierarchy in which grid cells are composed of multiple land units, snow/soil columns, and plant functional types (PFTs). Each grid cell can have a different number of land units, each land unit can have a different number of columns, and each column can have multiple PFTs. The vegetated land unit consists of a single column with up to four, out of a total of 17, PFTs occupying space on the column.

Biogeophysical processes are simulated for each subgrid land unit, column, and PFT independently, and include vegetation composition, structure, and phenology, the absorption, reflection, and transmittance of solar and longwave radiation, momentum, sensible and latent heat fluxes, ground evaporation, canopy evaporation, transpiration, canopy and soil hydrology, stomatal physiology and photosynthesis (Oleson *et al.*, 2004).

2.2 Data Used

The data used in the study consists of 1-year snapshots at 1990 and 2050, of land cover as simulated by a process-based terrestrial biogeochemistry model, TEM (Melillo *et al.*, 1993; Felzer *et al.*, 2004; Sokolov *et al.*, 2008), coupled to a CGE model of the world economy, the MIT EPPA model (Paltsev *et al.*, 2005; Gurgel *et al.*, 2007; and also described in Melillo *et al.*, 2009a).

The Melillo *et al.* (2009a) integrated modeling study used greenhouse gas emissions, as projected by EPPA, to drive a coupled atmospheric and climate module within the MIT Integrated Global System Model (IGSM), version 2.2 (Prinn *et al.*, 1999; Sokolov *et al.*, 2005) which simulates the future climate that then drives the TEM to simulate changes in crop, pasture, and forest productivity due to changing climate, levels of CO₂ and tropospheric ozone. These projected changes in productivity are then fed back to the EPPA model to change agricultural yields (Reilly *et al.*, 2007a), and along with changing demand for agricultural products, as driven by population and income growth, this leads to reallocations of land among uses, and conversions of land among land types (Melillo *et al.*, 2009a). These changes in land-use are fed back into the TEM to produce the land cover change data which is used in this study. As well as this output data from TEM, radiative forcing variables (trace gases (CO₂ etc.), aerosol concentration, the solar constant) from a 550 ppm stabilization scenario climate simulation by the IGSM were used in CAM to simulate the climate in 2050.

2.3 Modification of the Land Surface in CLM

In order to utilize the EPPA-IGSM-TEM derived land cover data we had to translate the IGSM-TEM land cover classification scheme, consisting of 34 land cover types (plus bare ground) to the CLM3.0 classification scheme, consisting of 16 PFT types (plus bare ground) required by the CLM3.0 input land surface dataset. **Table 1** lists the land cover types for both IGSM-TEM and CLM3.0.

Table 1. Land cover classification schemes for IGSM-TEM and CLM3.0.

Description of Land Cover Type	Code for PFT	IGSM-TEM	CLM
Bare ground	BG	0	0
Needleleaf evergreen tree (temperate)	NETTe	1	1
Needleleaf evergreen tree (boreal)	NETB	2	2
Needleleaf deciduous tree (boreal)	NDTB	3	3
Broadleaf evergreen tree (tropical)	BETTr	4	4
Broadleaf evergreen tree (temperate)	BETTe	5	5
Broadleaf deciduous tree (tropical)	BDTTr	6	6
Broadleaf deciduous tree (temperate)	BDTTe	7	7
Broadleaf deciduous tree (boreal)	BDTB	8	8
Broadleaf evergreen shrub (temperate)	BESTe	9	9
Broadleaf deciduous shrub (temperate)	BDSTe	10	10
Broadleaf deciduous shrub (boreal)	BDSB	11	11
C3 arctic grass	C3AG	12	12
C3 grass	C3G	13	13
C4 grass	C4G	14	14
Crop #1 (corn)	CR1	15	15
Crop #2 ('wheat', currently uncharacterised)	CR2	16	16
Wetlands tree (tropical)		17	
Wetlands no tree (tropical)		18	
Wetlands tree (temperate)		19	
Wetlands no tree (temperate)		20	
Wetlands tree (boreal)		21	
Wetlands no tree (boreal)		22	
Mangroves		23	
Coastal salt marsh		24	
Inland salt marsh		25	
Floodplains tree (tropical)		26	
Floodplains no tree (tropical)		27	

continued on page 7

Table 1 continued

Description of Land Cover Type	Code for PFT	IGSM-TEM	CLM
Floodplains tree (temperate)		28	
Floodplains no tree (temperate)		29	
Glaciers		30	
Lakes		31	
Rice paddies		32	
Pastures		33	
Urban		34	

In order to translate the IGSM-TEM land cover classification scheme to that required by CLM3.0, some decisions about how to reclassify the IGSM-TEM land cover types 18–35 had to be made. Since 100% of the IGSM-TEM land cover had to be accounted for in the reclassification process, some of the reclassifications were not ideal; for example, the IGSM-TEM classification scheme had several types of wetland, and with no equivalent CLM vegetation type, these wetland land cover types were reclassified as bare ground, even though this is clearly not a suitable category. There were other land cover types in IGSM-TEM which had no equivalent: land cover types 30, 31 and 34 are registered by the IGSM-TEM output dataset but they are not assigned any land area, so these have safely been recategorized as bare ground. Where an IGSM-TEM land cover type could be justifiably reclassified as more than one of the CLM PFTs, it has been split into two or more percentages of CLM PFTs (e.g. IGSM-TEM vegetation type #23 (mangroves) has been split evenly into constituting 50% of CLM PFT# 4, and 50% of CLM PFT# 5. **Table 2** details exactly how the 35 IGSM-TEM land cover types were translated into 17 CLM PFTs.

2.4. Modeling Scenarios

This study investigates the impact of large scale biofuel plantations on climate using two different economic land-use scenarios, or frameworks, as simulated by EPPA, which have the same economic growth and meet the same limit on industrial and fossil fuel greenhouse gas emissions. The two economic frameworks used in this study represent two economically plausible scenarios:

2.4.1. Pure Conversion Cost Response Model (PCCR)

This scenario (or framework) makes all land available for biofuels crops or other managed uses as long as the economic return on the land exceeds the cost of conversion and improvement. This scenario can be thought of as the “deforestation” or “extensification” scenario because it involves large-scale deforestation in support of biofuels production, either directly or indirectly. The direct link between deforestation and biofuels is when forests are cleared to establish

biofuels crops (Fargione *et al.*, 2008). The indirect link is when biofuel production moves on to croplands or pastures, and causes new forest clearing to relocate agriculture (Melillo *et al.*, 2009a).

Table 2. Converting from 35 TEM land cover/vegetation types to 17 CLM vegetation types.

CLM Land Cover Type	IGSM-TEM Land Cover Types Fitted to CLM Categories
Bare ground	Bare ground Wetlands no tree (tropical) + Wetlands no tree (temperate) + Wetlands no tree (boreal) + Floodplains no tree (tropical) + Floodplains no tree (temperate)
Needleleaf evergreen tree (temperate)	Needleleaf evergreen tree (temperate)
Needleleaf evergreen tree (boreal)	Needleleaf evergreen tree (boreal)
Needleleaf deciduous tree (boreal)	Needleleaf deciduous tree (boreal) + 0.5 * Wetlands tree (boreal)
Broadleaf evergreen tree (tropical)	Broadleaf evergreen tree (tropical) + 0.5 * Wetlands tree (tropical) + 0.5 * Floodplains tree (tropical) + 0.5 * Mangroves
Broadleaf evergreen tree (temperate)	Broadleaf evergreen tree (temperate) + 0.5 * Wetlands tree (temperate) + 0.5 * Floodplains tree (temperate) + 0.5 * Mangroves
Broadleaf deciduous tree (tropical)	Broadleaf deciduous tree (tropical) + 0.5 * Wetlands tree (tropical) + 0.5 * Floodplains tree (tropical)
Broadleaf deciduous tree (temperate)	Broadleaf deciduous tree (temperate) + 0.5 * Wetlands tree (temperate) + 0.5 * Floodplains tree (temperate)
Broadleaf deciduous tree (boreal)	Broadleaf deciduous tree (boreal) + 0.5 * Wetlands tree (boreal)
Broadleaf evergreen shrub (temperate)	Broadleaf evergreen shrub (temperate) + 0.5 * Coastal salt marsh + 0.5 * Inland salt marsh
Broadleaf deciduous shrub (temperate)	Broadleaf deciduous shrub (temperate)
Broadleaf deciduous shrub (boreal)	Broadleaf deciduous shrub (boreal)
C3 arctic grass	C3 arctic grass

continued on page 9

Table 2 continued

CLM Land Cover Type	IGSM-TEM Land Cover Types Fitted to CLM Categories
C3 grass	C3 grass + 0.5 * Coastal salt marsh + 0.5 * Inland salt marsh
C4 grass	C4 grass
Crop #1 (corn)	Crop #1 (corn) + Rice paddies + Pastures
Crop #2 ('wheat', currently uncharacterised)	*** BIOFUELS from IGSM-tem***

2.4.2. Observed Land Supply Response Model (OLSR)

This alternative scenario limits access to unmanaged land (e.g., tropical forests), with the limits based on the recent history of regional land conversion rates. This approach results in slower rates of deforestation than would be predicted by cost estimates alone (Gurgel *et al.*, 2007). This scenario can be thought of as the “intensification scenario” because one possible result of limited access to new land is that existing managed lands will be used more intensively, with increased inputs of capital, labor and materials such as fertilizers. For each scenario, the initial land cover distribution is based on the land cover distribution for the year 2000, which has been derived by reorganizing the gridded land-use transitions data sets of Hurtt *et al.* (2006) for use by TEM and EPPA (Melillo *et al.*, 2009a).

Both of these land-use trajectories consider two energy-policies: with and without the inclusion of cellulosic biofuel penetration into the global energy resource portfolio. Energy from cellulosic biofuels plays an important part in the global primary energy supply in 2050 in both scenarios where biofuels are included: 141 exajoules (EJ) yr⁻¹ in the deforestation scenario and 128 EJ yr⁻¹ in the intensification scenario. This is enough to meet at least 10% of the projected global energy requirement in 2050 (Melillo *et al.*, 2009a).

2.5. Experimental Design

A total of six simulations were done using the CAM3.1 model set-up, which are detailed in **Table 3**. These consisted of (1) a 1990 CLM simulation using the IGSM-TEM derived land cover types which have been reclassified into CLM PFTs (Table 2); both the climate forcing and land surface data are set to 1990. Simulation (2) was conducted with the climate forcing set to 2050 conditions (i.e. information about the aerosol forcing, CO₂ concentrations, etc.), and the land surface data set to 1990 conditions, with the aim of comparing this simulation to (1) in order to isolate the impact of the atmospheric forcing alone. Simulations (3) to (6) were conducted with both the climate forcing and the land surface dataset set to 2050 conditions, for each of the four scenarios—two simulations each for the PCCR and OLSR economic frameworks, one with a cellulosic biofuel-based energy policy implemented in 2026 in the original IGSM-TEM data, and one where this energy policy is not implemented.

The results of these simulations were used in a series of analyses designed to show the climate impact of land cover change from 1990 to 2050, for each of the four scenarios in 2050, and then to elucidate the causes of the changes. These analyses are listed in **Table 4**. In order to compare the biogeophysical surface temperature this global biofuel energy policy with the results of Melillo *et al.* (2009) which show the biogeochemical temperature response, another two CAM simulations were conducted which added onto the default CO₂ used by CAM3.1 the total (i.e. direct and indirect) carbon gain (or loss) to the atmosphere (in ppmv CO₂) from both the deforestation-with-biofuels (i.e. PCCR) and intensification-with-biofuels (OLSR) scenarios, as calculated by Melillo *et al.* (2009), minus a fraction (approximately 20%, derived from IGSM simulations) of CO₂ which is taken up by the terrestrial biosphere. As such, the biogeochemical impacts on global surface temperature can be isolated and then compared to the biogeophysical impacts in a realistic way.

Table 3. CAM3.1 Simulations.

Simulation	Name	land cover at year	Trace gas (atmospheric) forcing at year	Economic framework	Biofuels policy	Purpose
1	'temls1990'*	1990	1990	None	None	Control for policy runs
2	's50t90'**	1990	2050	None	None	Compare to policy runs to isolate land cover change
3	'pccr'	2050	2050	PCCR	Yes	Analyze biofuels impact
4	'pccr-nb'	2050	2050	PCCR	None	Compare to biofuels case
5	'olsr'	2050	2050	OLSR	Yes	Analyze biofuels impact
6	'olsr-nb'	2050	2050	OLSR	None	Compare to biofuels case
7	'pccr + extra CO ₂ '	2050	2050	PCCR	Yes	Analyze impact of CO ₂ emitted as a result of biofuels policy
8	'olsr + extra CO ₂ '	2050	2050	PCCR	Yes	Analyze impact of CO ₂ emitted as a result of biofuels policy

* (Atmosphere at 1990, TEM land Cover at 1990)

** (Atmosphere at 2050, TEM land cover at 1990)

Table 4. Analyses performed using results of 6 CAM3.1 simulations.

Analysis	The difference of 2 simulations:	Shows impact of:
1	's50t90' – 'temls'	Climate change (from 1990 to 2050) only: the land cover is held constant
2	'PCCR ' – 's50t90'	Land cover change only (in the PCCR-biofuels scenario)
3	'PCCR-NB ' – 's50t90'	Land cover change only (PCCR-no biofuels scenario)
4	'OLSR ' – 's50t90'	Land cover change only (OLSR-biofuels scenario)
5	'OLSR-NB ' – 's50t90'	Land cover change only (OLSR-no biofuels scenario)
6	'PCCR ' – 'temls'	Land cover change + climate change (PCCR biofuels)
7	'PCCR-NB ' – 'temls'	Land cover change + climate change (PCCR, no biofuels scenario)
8	'OLSR ' – 'temls'	Land cover change + climate change (OLSR biofuels)
9	'OLSR-NB ' – 'temls'	Land cover change + climate change (OLSR, no biofuels)
10	'PCCR' – 'OLSR'	Economic framework, with biofuels
11	'PCCR' – 'PCCR-NB'	Biofuels in the PCCR framework
12	'PCCR+extra CO ₂ ' – 'PCCR'	CO ₂ from biofuels in the PCCR framework
13	'OLSR+extra CO ₂ ' – 'OLSR'	CO ₂ from biofuels in the OLSR framework

3. RESULTS AND DISCUSSION

The different economic frameworks and the implementation of a biofuel energy policy changes the distribution of land cover, including vegetation types, and alters the reflectivity of the land surface. This changes the amount of energy available at the surface to heat the atmosphere and evaporate water, which impacts climate on local to global scales. The following analysis will differentiate the impact on climate of the four different economic framework/biofuel policies, and also in terms of the impact from just land cover change (LCC)

alone, as well as the impact from LCC combined with the impact of radiative forcing. Lastly, a comparison is made of the biogeophysical and biogeochemical impacts of land-use change due to biofuels.

3.1 IGSM-TEM Land Cover Change from 1990 to 2050: 4 Scenarios

An analysis of the changes in percent PFT between 1990 and 2050 for all four land-use/policy scenarios reveals that one-third of the PFTs showed no or only very minor changes over this period (defined as no changes anywhere which exceeded 10%), and that in the PCCR scenarios there were fewer PFTs which changed so little; these were PFTs 1 (bare ground), 6 (broadleaved evergreen tree, temperate), 9 (broadleaved deciduous tree, boreal), 10 (broadleaved evergreen shrub, temperate) and 13 (C3 Arctic grass). In both the OLSR scenarios, with and without biofuels, there were 8 PFTs showing such trivial changes: PFTs 1 (bare ground), 4 (needleleaf deciduous tree, boreal), 6 (broadleaf evergreen tree, temperate), 9 (broadleaf deciduous tree, boreal), 10 (broadleaf evergreen shrub, temperate), 12 (broadleaf deciduous shrub, boreal), 13 (C3 Arctic grass) in the case of OLSR and 7 (broadleaf deciduous tree, tropical). In the OLSR-without-biofuels scenario, PFT 2 (needleleaf evergreen tree, temperate) also showed very little change.

In both of the PCCR scenarios there were many PFTs which showed major changes (defined as a change anywhere in the world which exceeded 20%). These PFTs were 3 (needleleaf evergreen tree, boreal), 4 (needleleaf deciduous tree, boreal), 5 (broadleaf evergreen tree, tropical), 11 (broadleaf deciduous shrub, temperate), 14 (C3 grass), 15 (C4 grass), 16 (crop 1) and 17 (crop 2, i.e. biofuels). In terms of both spatial extent and percentage change, the PFTs which showed the most change were both of the crop PFTs (16 and 17), PFTs 5 (broadleaf evergreen tree, tropical) and 7 (broadleaf deciduous tree, tropical) in the tropics, PFTs 3 and 4 (needleleaf evergreen and deciduous trees, boreal) in the boreal zone and PFT 11 (broadleaf deciduous shrub, temperate) in the temperate latitudes. The PFTs which showed major changes in the OLSR-with-biofuels were PFTs 3, 5, 7, 14, 15, 16, and 17. The absence of biofuels results in much less of a change in PFTs 7 and 15. These percent PFT changes for all four scenarios are shown in **Figure 2a-2d**. A visual analysis of these maps indicates that the biofuels grown in the PCCR scenario (i.e. “crop 2”) replace, to some extent, PFTs 8, 5, 11, and 14, and PFT 15 to a lesser extent also. Crop 1 (non-biofuels cropland) replaces PFTs 11, 3, 5 (in Africa), 7 and 14. In the OLSR scenario, it is apparent that a lot of the biofuel crop is replacing (or perhaps displacing) crop 1 (PFT 16), particularly in Africa and South America, whereas in the PCCR scenario there is greater (i.e. higher percentage) replacement of crop 1 in north America, and biofuel growth in Eurasia—replacing PFT 3 (needleleaf evergreen tree, boreal).

3.2. The Impacts of Different Land-Use and Biofuels Policies on the Surface Climate

In order to understand the global impact of changing the land cover according to the four land-use and biofuel scenarios, the global 50 year annual mean (weighted for latitude) was calculated for the variables of interest, discussed below. Their global annual means are listed in Table 5.

3.2.1. Albedo, Net Radiation and the Surface Energy Balance

The change in land cover as a result of implementing a global-scale biofuels-based energy policy leads to marked changes in the reflectivity of the land surface, or albedo, in the PCCR and OLSR scenarios that incorporate biofuels (**Figure 3**). Generally speaking, cropland has a higher albedo (α) than the forested land. This has the effect of changing the radiation budget of the land surface, which can be written as:

$$R_n = (1 - \alpha)SW + ILW - OLW \quad (1)$$

where R_n = net radiation, SW = incoming solar radiation, ILW = incoming longwave radiation, and OLW = outgoing longwave radiation. Albedo has a direct influence on net radiation and therefore determines how much energy is available at the surface for partitioning into the latent, sensible and ground (soil) heat fluxes, called the energy balance, which is a major determinant of land-surface temperature, the equation for which can be written as:

$$C \frac{dT}{dt} = R_n - LH - SH - G - A \quad (2)$$

where SH = sensible heat flux, LH = latent heat flux, G = ground heat flux, T = temperature of land surface, C = heat capacity of the land surface, and A = energy advection (Oke, 1987). Energy advection (A) is not considered here, as it is assumed to be of negligible influence. Among the land-use scenarios considered, the largest changes in albedo occur for the PCCR case (Figure 2), which is due to the greater extent of deforestation in this economic framework controlling land-use, and also due to the greater extent of cropland grown of all the four scenarios considered in this study (also in terms of the intensity of plantations within the areal extent of cropland). Specifically, for the PCCR-without-biofuels case, large areas of increased albedo in the high northern latitudes are seen (Figures 2c and 2d), with the strongest increases over Siberia where large areas of needleleaf evergreen tree (boreal) have been deforested. By comparison, for the OLSR case (Figures 2e and 2f) these albedo increases in the high northern latitudes are absent.

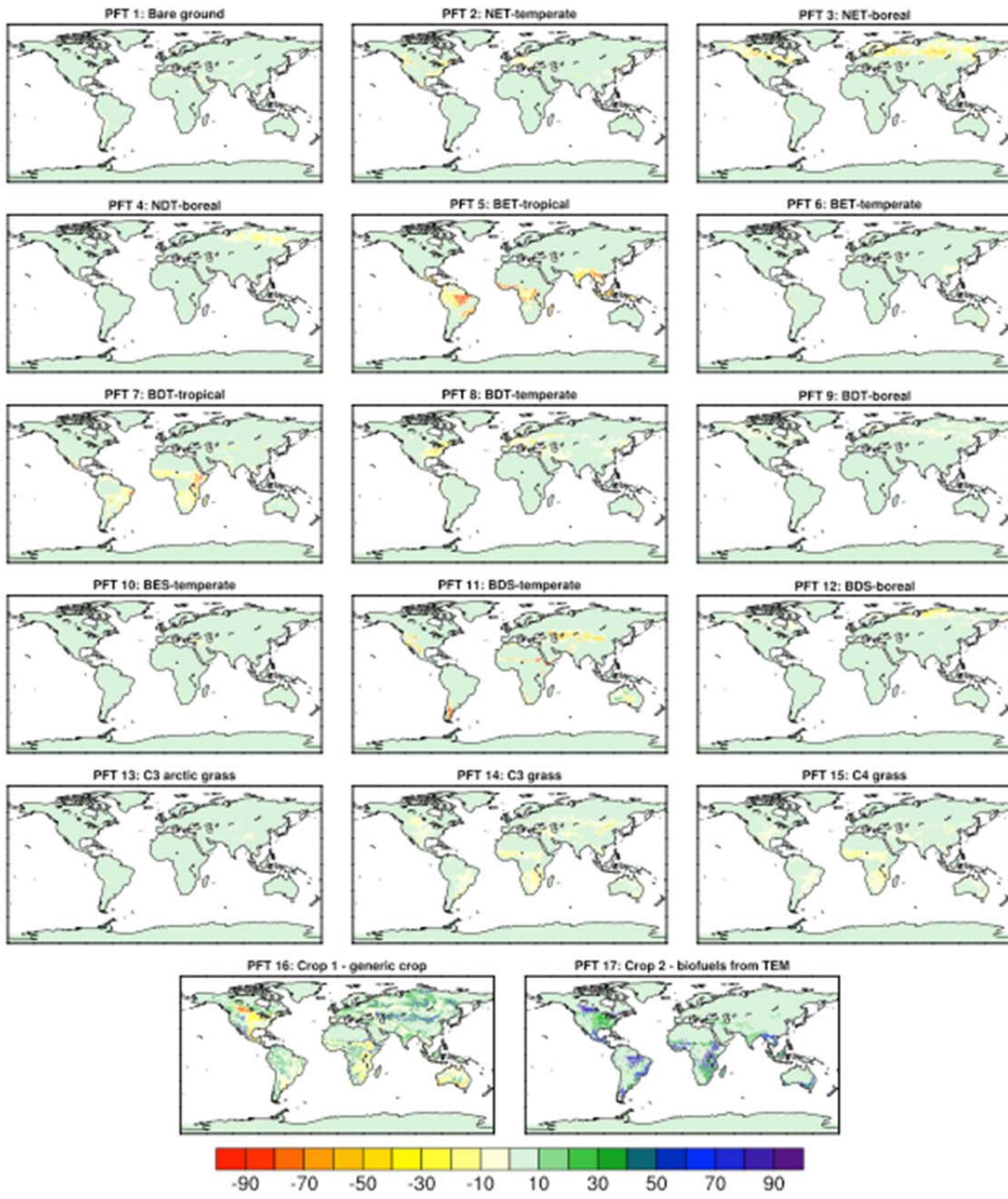


Figure 2 (a). Maps showing the percent change over time in the PCCR-with-biofuels scenario.

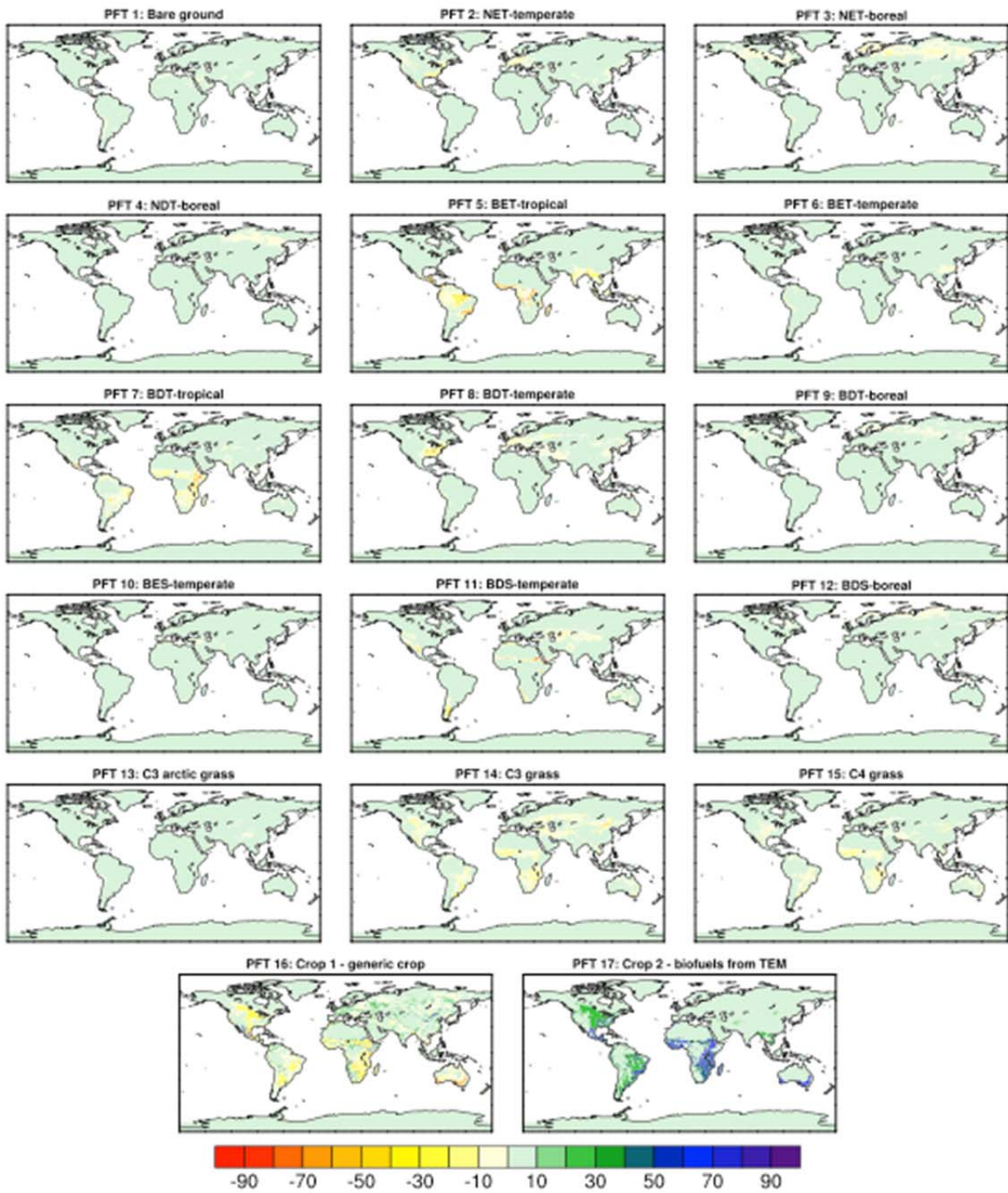


Figure 2 (b). Maps showing the percent change over time in the OLSR-with-biofuels scenario.

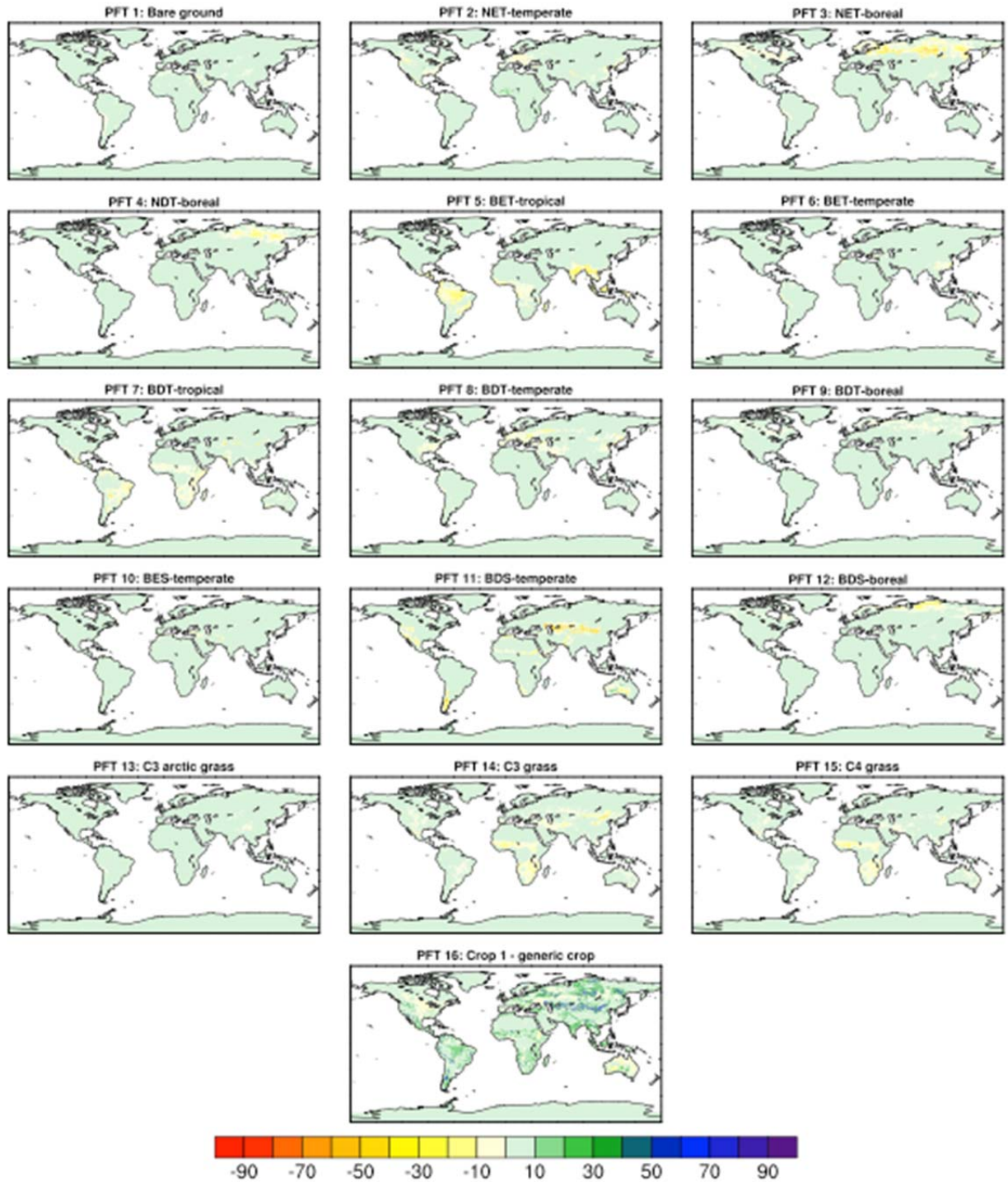


Figure 2 (c). Maps showing the percent change over time in the PCCR-without-biofuels scenario.

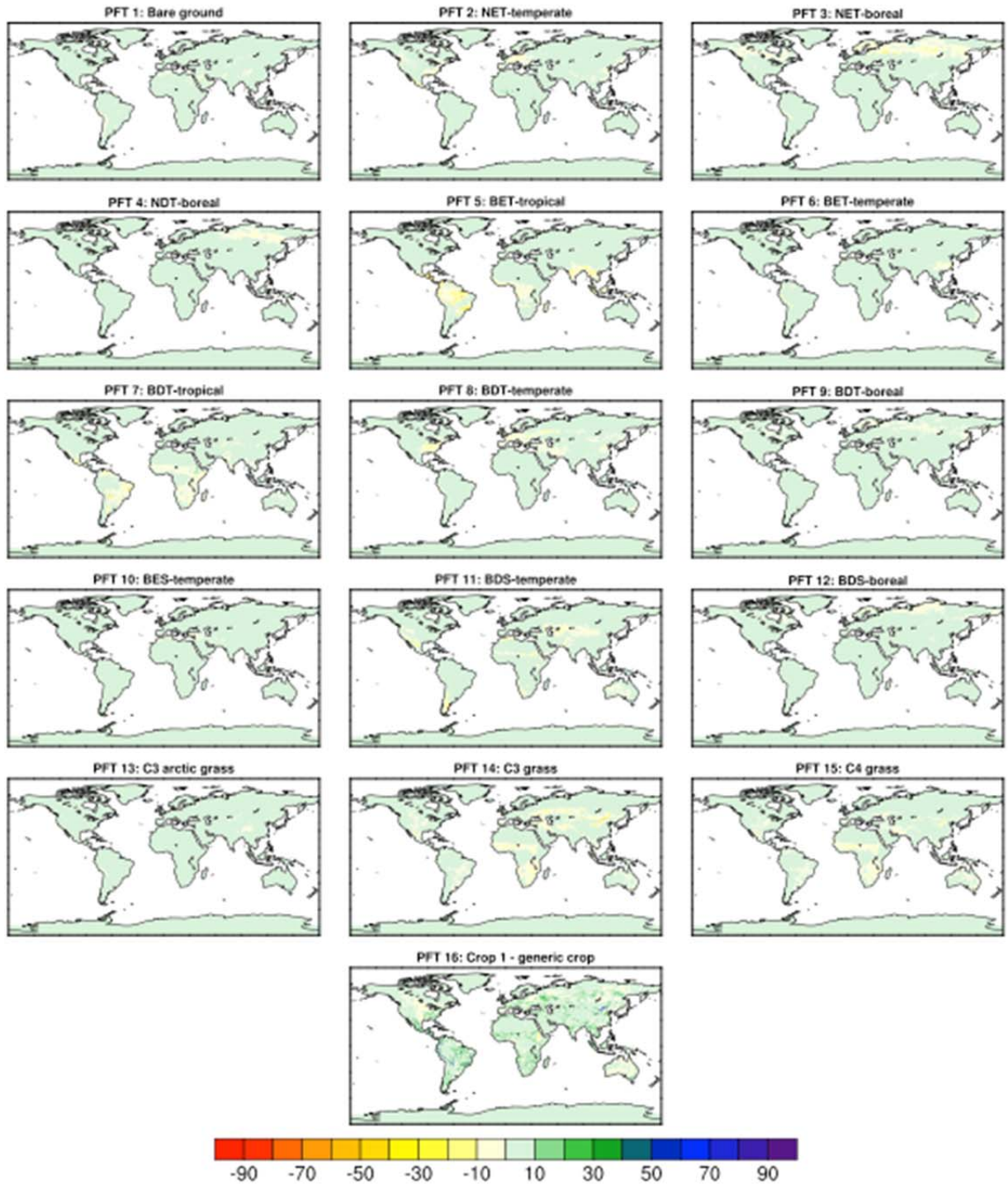


Figure 2 (d). Maps showing the percent change over time in the OLSR-without-biofuels scenario.

* The percent PFT maps for 1990 and the four land-use/biofuels scenarios are in Appendix 1.

Table 5. Weighted Global 50-year Annual Means for albedo, surface temperature and energy balance terms (changes from 1990-2050, and absolute values).

Variable	Units	Scenario	Absolute Value	Change due to CC only	Change due to LCC only	Overall change, CC+LCC
Global Albedo	(fraction)	Ext. with biofuels	0.240	-0.003	0.012	0.009
		Ext. without biofuels	0.233		0.005	0.002
		Int. with biofuels	0.234		0.006	0.003
		Int. without biofuels	0.230		0.003	-0.001
2m surface temperature	K	Ext. with biofuels	288.256	0.751	-0.258	0.493
		Ext. without biofuels	288.375		-0.139	0.612
		Int. with biofuels	288.368		-0.146	0.605
		Int. without biofuels	288.466		-0.048	0.703
Latent heat flux	W m ⁻²	Ext. with biofuels	83.642	1.090	-0.503	0.590
		Ext. without biofuels	83.926		-0.219	0.871
		Int. with biofuels	83.851		-0.293	0.800
		Int. without biofuels	84.114		-0.030	1.060
Sensible heat flux	W m ⁻²	Ext. with biofuels	17.568	-0.401	-0.146	-0.550
		Ext. without biofuels	17.638		-0.075	-0.476
		Int. with biofuels	17.619		-0.094	-0.500
		Int. without biofuels	17.639		-0.074	-0.475
Surface net radiation	W m ⁻²	Ext. with biofuels	505.466	4.465	-1.876	2.589
		Ext. without biofuels	506.379		-0.963	3.502
		Int. with biofuels	506.231		-1.111	3.354
		Int. without biofuels	507.020		-0.322	4.143

The increase in albedo seen in Eurasia from 1990 to 2050, for both the PCCR and OLSR-with-biofuels scenarios, is due to the increase of the 'generic' (i.e. non-biofuels) crop PFT found in CLM3.0, and not due to an increase in the area of biofuel cropland. This is the case for all four policy scenarios, however the generic cropland does not show as great a northerly extension in the OLSR scenarios as it does in the PCCR scenarios. Moreover, the greater albedo changes (and greater cooling, discussed below) in these high northern latitudes seen in the PCCR case (compared to the OLSR case) is due to the greater intensity of this new crop growth in these newly cultivated northern croplands in Eurasia, as well as the new areas of biofuel growth in North America in 2050, the intensity of which is much higher in high northern latitudes of the

PCCR case compared with OLSR case. This accounts for the noticeably higher albedo in North America in the PCCR case.

Percent PFT maps are shown in the Appendix (**Figure A.2**) which illustrate the changes over time from 1990 to 2050 of the extent of ‘generic’ cropland in CLM, as well as the differences between the two economic frameworks in terms of both the generic cropland and the biofuels present in 2050. There is much more cropland in the far north of Eurasia in the PCCR scenario, and much more biofuel cropland in North America also, and it is this addition of areas of both non-biofuel and biofuel cropland in the high northern latitudes (seen from changes in percent PFTs from 1990–2050, shown in Figure 2a) which, as this report will show, plays such an important role in regional albedo, and which has led to the climate impacts described in this study. Figure 3a shows the impact of changes in radiative forcing on the albedo of the land surface between 1990 and 2050. The albedo changes are the same for all scenarios because the climate/radiative forcing was the same for all simulations.

Therefore the albedo changes seen which incorporate the impact of land cover change and the change in radiative forcing are not shown, since they are almost identical to those which show just the impact of land cover change (Figures 3c–3f). Figure 3c shows that the PCCR-with-biofuels scenario, and the deforestation it entails, is the land-use/energy policy that leads to the strongest albedo increases in the high northern latitudes. We assess the different impacts of the land-use and energy policies on albedo by considering the differences between both the PCCR and OLSR scenarios (both have biofuels), and the PCCR-with- and PCCR-without-biofuels scenarios (Figure 3b and 3g). The latter (3g) shows an increase in albedo only in parts of North America but not Eurasia, and illustrates an albedo change which is attributable to the biofuels (i.e. energy) policy but not the economic framework controlling land-use. The PCCR-OLSR result shows albedo increases in both North America and Eurasia, and indicates that the land-use policy contributed to the land cover change, and subsequent albedo increase, over Eurasia.

The increase in albedo (red) in the northern hemisphere can be accounted for by increase in ‘generic crop land’ and biofuels in North America and Eurasia which have replaced other PFTs, as already discussed above. The decrease in albedo in northern Australia between 1990 and 2050 in the PCCR scenarios is likely accounted for by a decrease in generic crop. In the OLSR scenario, biofuel cropland replaces ‘generic’ cropland to a large extent compared to the PCCR scenario.

This would contribute to the lesser changes in albedo seen in the OLSR scenarios (compared to the PCCR scenarios) in South America and Africa where the majority of the biofuel cropland is located, due to the fact that the CLM3.1 prescription of ecophysiological parameter values for generic crop and biofuels are identical (the implications for which will be addressed in the closing section).

The primary effect of albedo change is to alter the amount of net radiation at the surface, and this will lead to changes in energy available for sensible heat flux and evapotranspiration (latent heat flux). There is a marked decrease in surface net radiation from 1990 to 2050 in the PCCR (**Figure 4a**) and PCCR-NB (Figure 4b) scenarios, which covers most of Eurasia and scattered

areas of South America and a non-local decrease over the Arctic Ocean in both cases, and all of North America in the PCCR case as well. In the OLSR scenarios, there is less impact on the Arctic Ocean, but the OLSR-with-biofuels scenario shows major decreases in the USA and Mexico, as well as the parts of Africa also affected in the PCCR scenario as well, indicating that it is the biofuel policy and not land-use policy which is responsible for this result. The land areas which show reduced net radiation clearly correspond with those areas in North America and Eurasia where albedo increases.

A change in net radiation can lead to a change in temperature, as given by equations (1) and (2), but the partitioning of the net radiation between latent and sensible heating depends on the moisture at the surface, which can also influence temperature. To assess how the altered net radiation was partitioned between the turbulent heat fluxes at the surface, the evaporative fraction (EF) was calculated for all four policy/land-use scenarios as follows;

$$EF = \frac{LH}{LH + SH} \quad (3)$$

There are large areas of northern South America (including a large part of the Amazon basin) and Africa in the PCCR LCC-only maps which show a decrease in EF, as well as areas in North America and Eurasia which show an increase in EF (**Figure 5**). Over much of North America it is the larger decrease in sensible heat flux (**Figure 6c**) more than the smaller increase in latent heat flux (not shown) that increases EF up to 0.1 (in the case of the change in PCCR from 1990–2050), as shown in Figure 5a.

If EF remains unchanged, a decrease in net radiation will result in a decrease in the surface temperature due to a concomitant decrease in the surface sensible heat flux. This is what is seen over much of the northern hemisphere land mass (Figure 6). The mechanism to explain the decrease in temperatures (from 1990 to 2050) over much of the northern hemisphere is the decrease in albedo and subsequent surface net radiation reduction (Figure 4a). However, there is an increase in EF over many parts of North America and Eurasia in the PCCR-with-biofuels scenario, as seen in Figure 5a (and over Eurasia only, in the PCCR-without-biofuels scenario) that compounds this decrease in surface radiation and lowers temperatures further.

A decrease in EF, seen in the parts of the Amazon region and Africa is accompanied by an increase in sensible heat flux and subsequent surface temperature rise, as seen in the PCCR-with-biofuels scenario (Figure 6a). The difference between the response to deforestation in much of the tropics (i.e. increase in sensible heat flux and temperature) compared to the extratropics (general decrease in sensible heat flux and temperature) occurs because tropical forests maintain high rates of evapotranspiration, which offsets the surface warming from the low albedo of forests (Bonan, 2008).

Therefore, with deforestation, albedo increases in many parts of the tropics, but instead of this leading to a cooling (due to lower net radiation), it leads to a warming due to the disruption in evaporative cooling provided by forest hydrology, once deforestation takes place.

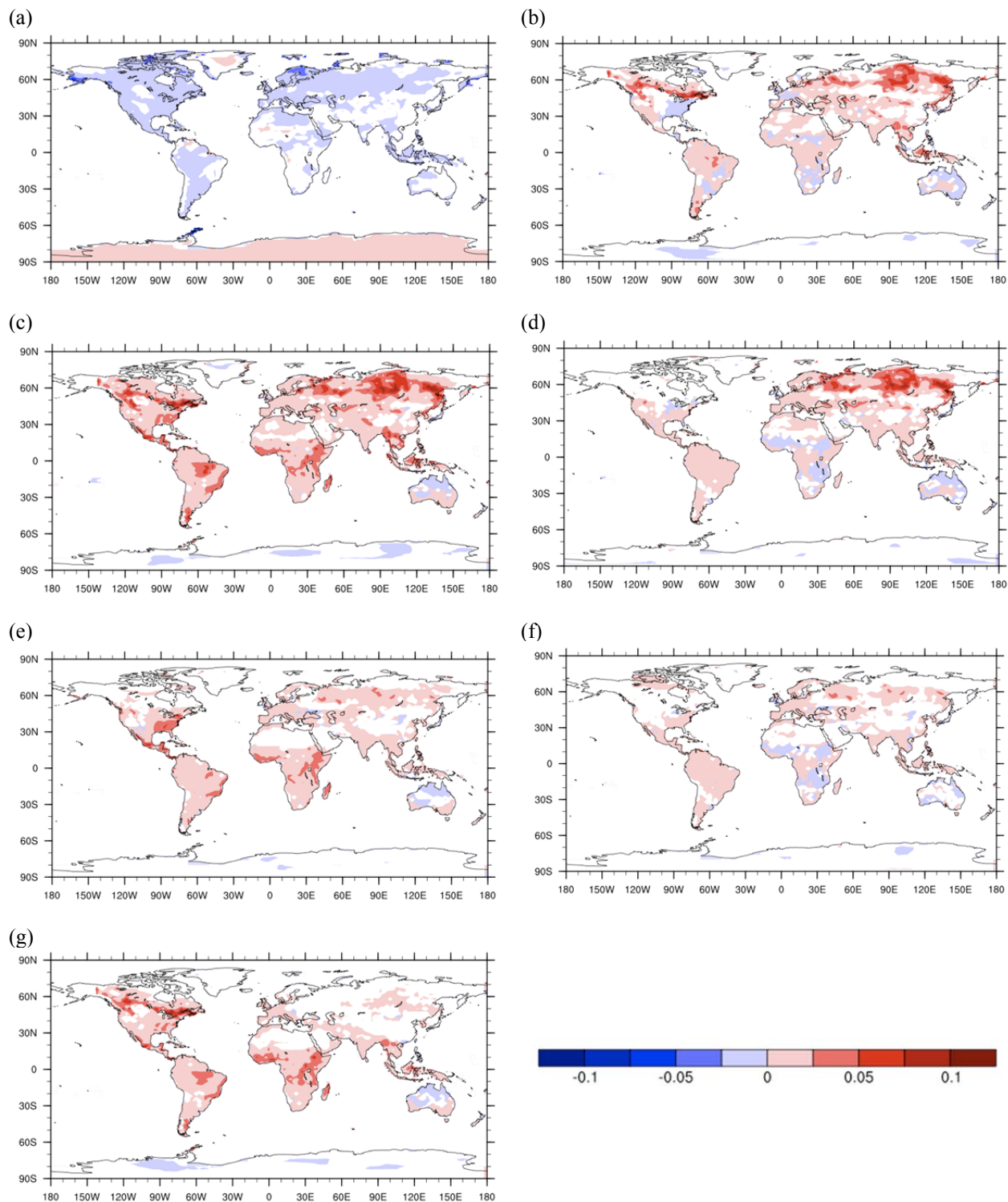


Figure 3. Changes in land surface albedo (unitless) from 1990 to 2050 for (a) just the greenhouse effect, (b) the difference between the PCCR-OLSR scenarios (with biofuels), (c) changing only the land cover in the PCCR scenario, with biofuels, and (d) without biofuels, (e) changing only the land cover in the (continued on page 22)

(continued from page 21)

OLSR scenario with biofuels, and (f) without biofuels, (g) just the difference between the presence and absence of biofuels in the PCCR scenario. Non-shaded areas denote statistically insignificant results ($p > 0.05$).

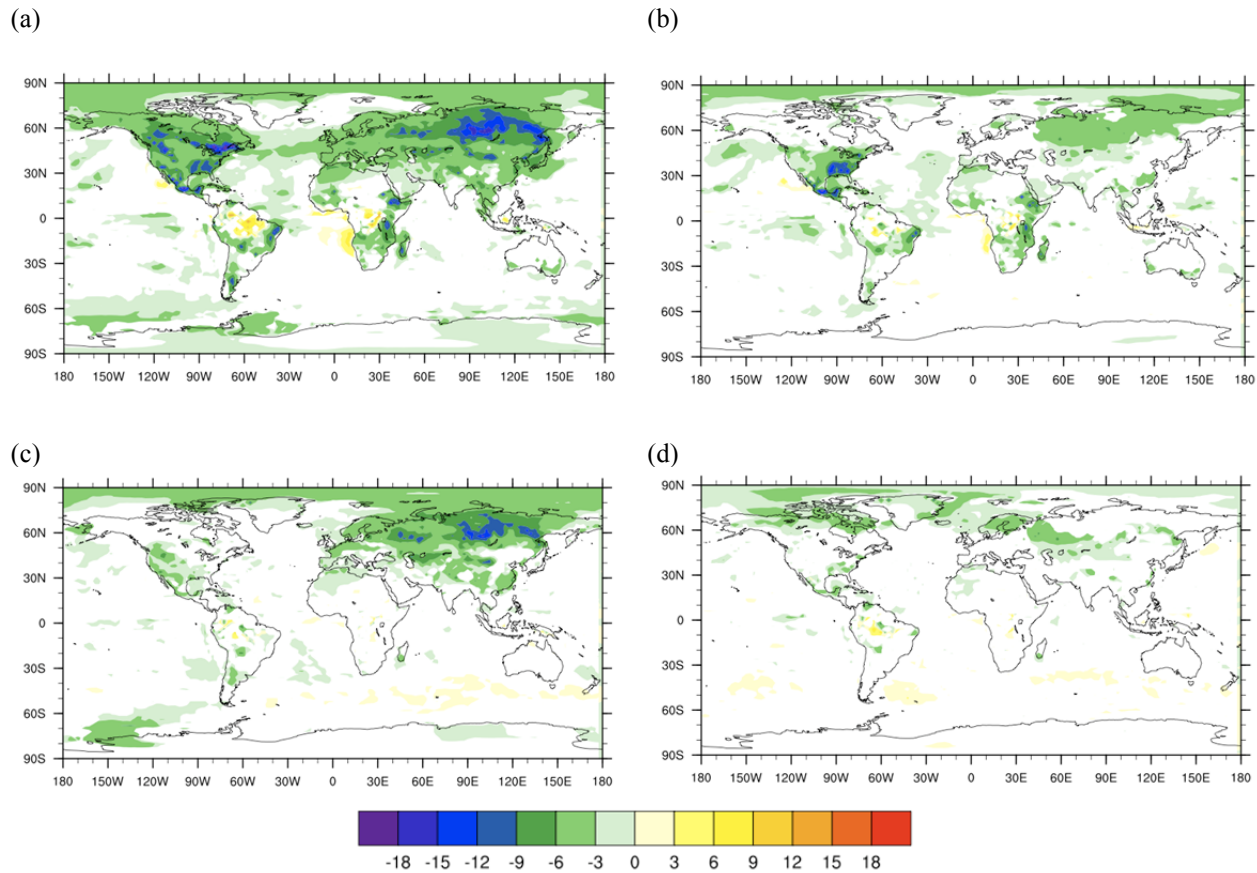


Figure 4. Surface net radiation (W m^{-2} , change from 1990 to 2050), in (a) the PCCR and (b) OLSR, (c) the PCCR-no biofuels scenarios, and (d) the OLSR-no biofuels scenarios, in terms of the impact of LCC only. Non-shaded areas denote statistically insignificant results ($p > 0.05$).

If the forest is cut down and replaced by crop or pasture, then the evaporative fraction can change in response to ecophysiological changes of the new land cover. For example, the replacement of most vegetation types with crops acts to decrease leaf area index (LAI) and rooting depth, which decreases the capacity to transpire moisture from the soil, lowering canopy evaporation, and reducing access to deeper soil water. Also a lower canopy height will reduce the turbulent transfer of heat to the atmosphere, (e.g., Pitman *et al.*, 2009) all of which leads to less evaporative cooling. Both modeling and flux tower studies confirm that in the Brazilian Amazon, forests have lower albedo compared with pasture, greater net radiation, and greater evapotranspiration, particularly during the dry season. The same processes have been found to occur in the tropical forests of Africa and Asia (Bonan, 2008).

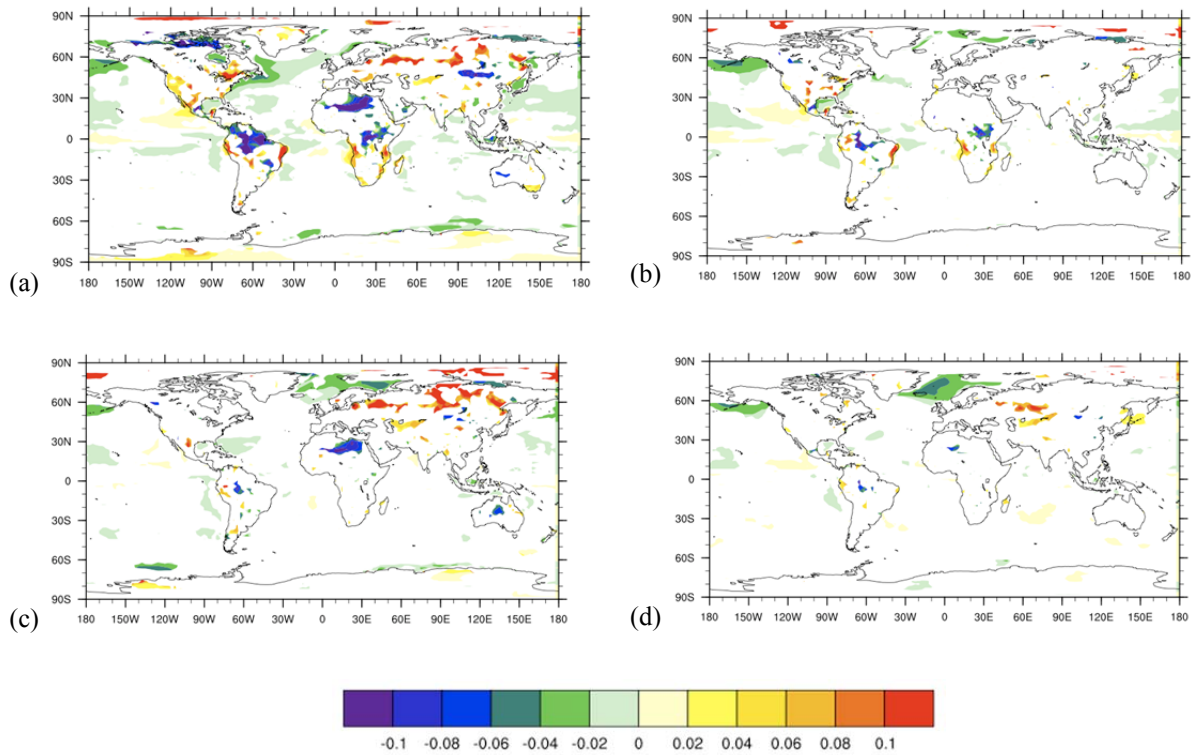


Figure 5. Evaporative Fraction (unitless); Impact of just Land Cover Change, in the four scenarios: (a) PCCR with biofuels, from 1990 to 2050, (b) OLSR with biofuels, (c) PCCR without biofuels and (d) OLSR without biofuels. Non-shaded areas denote statistically insignificant results ($p > 0.05$).

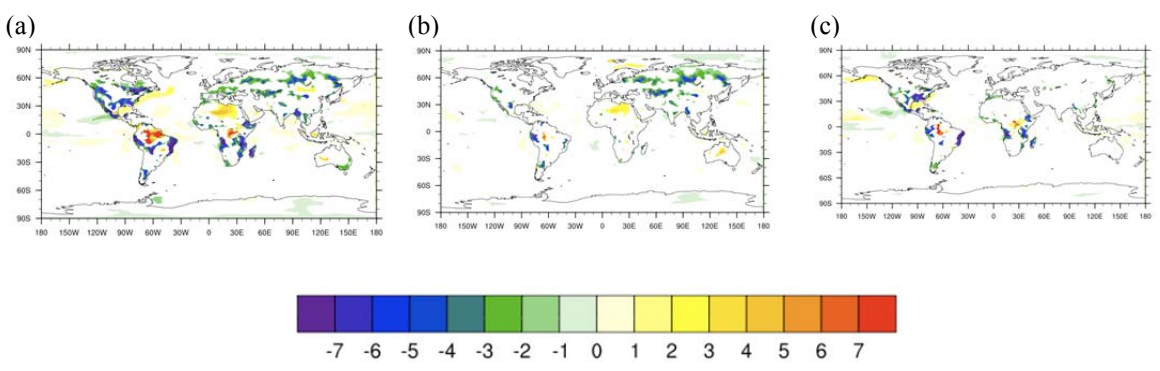


Figure 6. Impact of just Land Cover Change on Sensible Heat Flux ($W m^{-2}$) for the (a) PCCR scenario with biofuels, (b) PCCR scenario without biofuels, (c) OLSR scenario with biofuels. Non-shaded areas denote statistically insignificant results ($p > 0.05$).

The cause of the lower latent heat flux and higher sensible heat flux, and areas of warmer temperatures in the tropical regions, discussed below, are likely due to changes in canopy evaporation (**Figure 7**) and transpiration (**Figure 8**). There are large areas of decreased canopy evaporation and transpiration in the tropics, in the areas of meso- and northern South America, tropical Africa and southern and southeast Asia (with the greatest changes seen in the Amazon region) for the PCCR scenario (Figures 7a and 8a), with smaller decreases in the OLSR scenario, and other non-biofuels scenarios (not shown). The canopy evaporation and transpiration decrease most in the biofuels scenarios, in terms of area of land where this occurs, however the PCCR economic framework causes the largest decline in the areas where there are decreases in canopy evaporation and transpiration, particularly in The Amazon Basin and southeast Asia.

The spatial changes in ground evaporation in the tropics, likely due to the more open canopy of cropland and other vegetation types which have replaced the original vegetation type, correspond quite well with the areas where biofuels are grown. Unsurprisingly, this is most apparent in the PCCR scenario (Figure 8d) in places like the Amazon basin, where there was very intensive (i.e. large percentage) deforestation and replacement with biofuels; it exists but is much less pronounced in the other three scenarios. However, this source of moisture (ground evaporation) is not enough to prevent decreases in the evaporative fraction in parts of the Amazon basin and tropical Africa in the face of the deforestation in the PCCR scenario (Figure 5a).

The most salient land areas where net radiation increases due to LCC alone are the Amazon region and central Africa as seen in the PCCR scenario (Figure 4a). However, the increase in albedo seen (Figure 3c) in Africa, which should lower net radiation, seems to be inconsistent with the net radiation increase. However, an analysis of cloud cover—particularly low cloud cover over the Amazon and central African regions corresponding to the area of increased surface radiation—shows there is a marked decrease in cloud cover, indicating that the increase in net radiation is due to increased insolation due to less cloud cover, rather than just changes in albedo alone (Figure 9a).

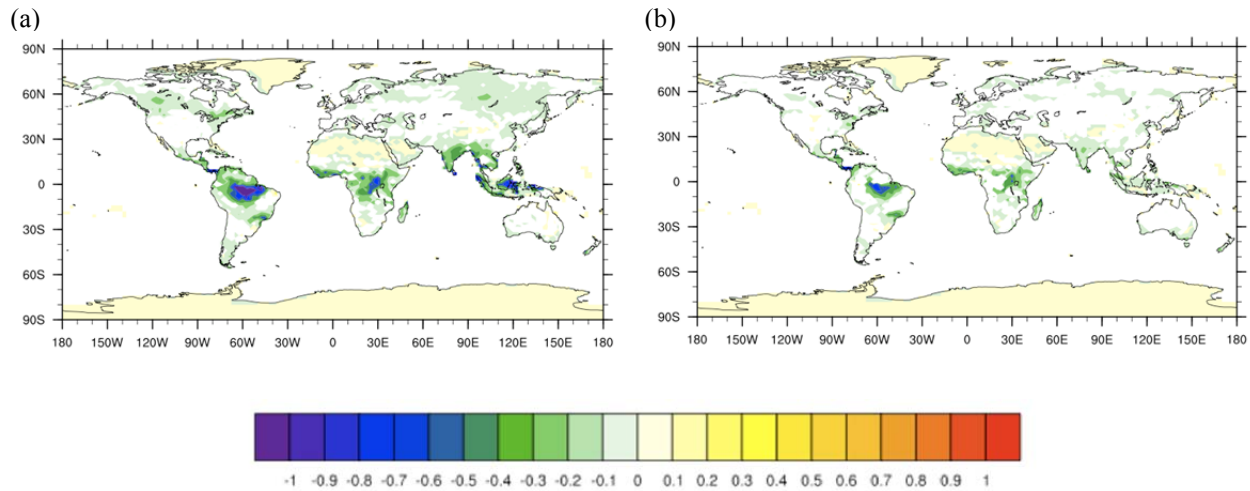


Figure 7. Canopy evaporation ($W m^{-2}$) for the biofuel policy scenarios: (a) PCCR-with-biofuels, (b) OLSR-with-biofuels. Non-shaded areas denote statistically insignificant results ($p > 0.05$).

This occurs to a much smaller extent in the OLSR case also (Figure 9b). This decrease in cloud cover does not occur in either of the PCCR-without-biofuels (except for relatively smaller increases in low cloud over western Eurasia (not shown)) or OLSR-without-biofuels scenarios, (not shown) and an analysis of the difference between PCCR-with and PCCR-without-biofuels scenarios (Figure 9c) and the PCCR vs. OLSR scenario (Figure 9d) makes clear that it is the combination of the PCCR and biofuels policy which responsible for the most dramatic changes.

The statistically significant areas of greater low cloud cover in Eurasian and North American extratropics would also likely be contributing to the decrease in net radiation over these areas in the case of the PCCR scenarios (in terms of changes due to LCC only).

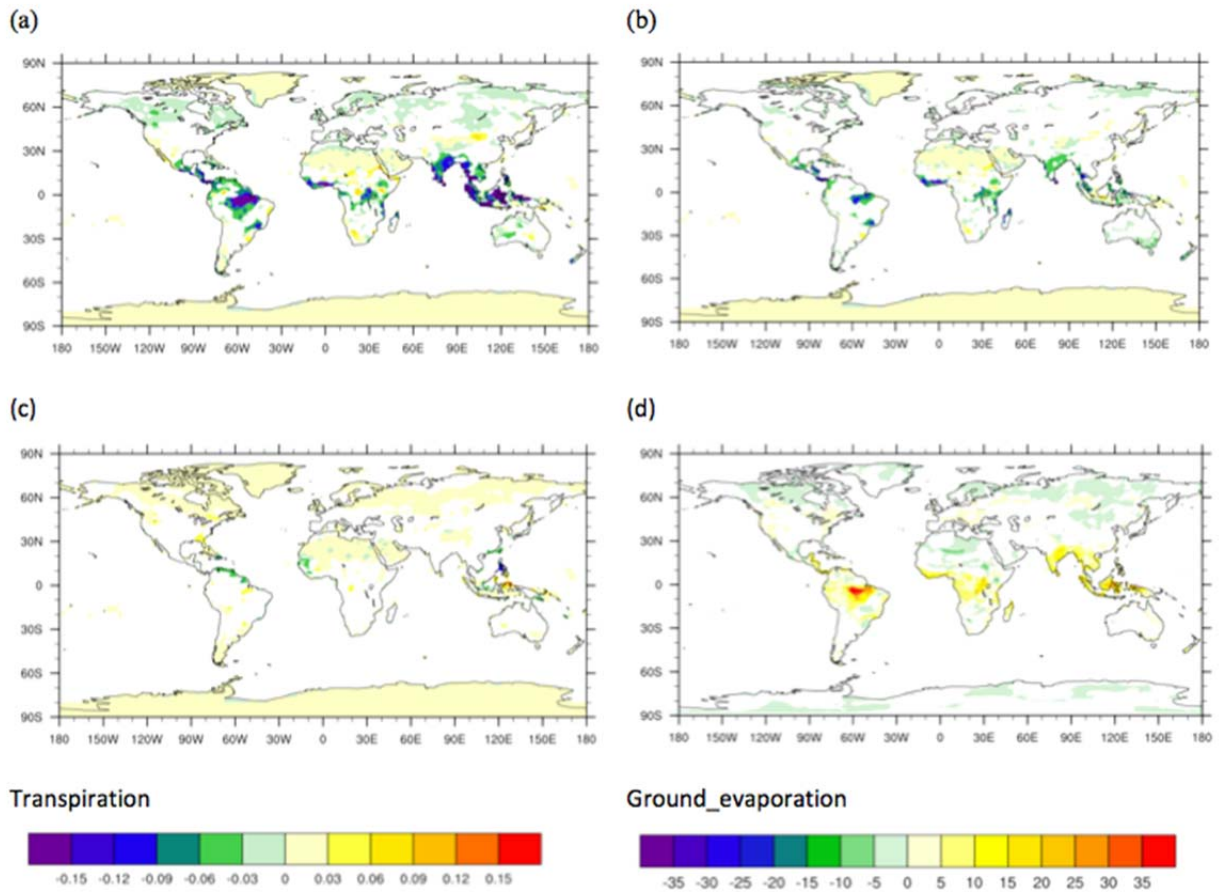


Figure 8. Transpiration (mm/s) for three scenarios: (a) PCCR-with-biofuels, (b) OLSR-with-biofuels, (c) Impact of just Climate Change 1990 to 2050, and (d) Ground evaporation (W m^{-2}) for the PCCR-with-biofuels scenario. Non-shaded areas denote statistically insignificant results ($p > 0.05$).

3.2.2. Temperature: The Integrated Response

From the land-use scenarios considered, the impact of albedo change on the surface radiative and turbulent heat fluxes is not entirely straightforward. As shown, the climate forcing (i.e. heating or cooling) of forests differs by latitude, and is mediated by the role that the forests in different latitudes play in the regional hydrological cycle (e.g., Bonan, 2008). As this report has shown, changes in surface net radiation can arise from changes in albedo as well as cloud cover, but that low cloud cover appears to be a more salient factor in the changes in net radiation over the tropics in this study.

Bonan (2008) indicates that the large-scale conversion of tropical forest to pasture creates a warmer, drier climate, which goes against the general rule that an increase in albedo (such as is to be expected in the case of Amazonian deforestation) leads to a decrease in net radiation at the surface and therefore a decrease in the energy available for partitioning into sensible heat, which decreases surface air temperature. The simulated changes in surface-air temperature and

evaporative fraction from 1990 to 2050 in the PCCR scenario (**Figure 10c**) indicate that there is just such an area of higher temperatures and drier conditions in the Amazon basin.

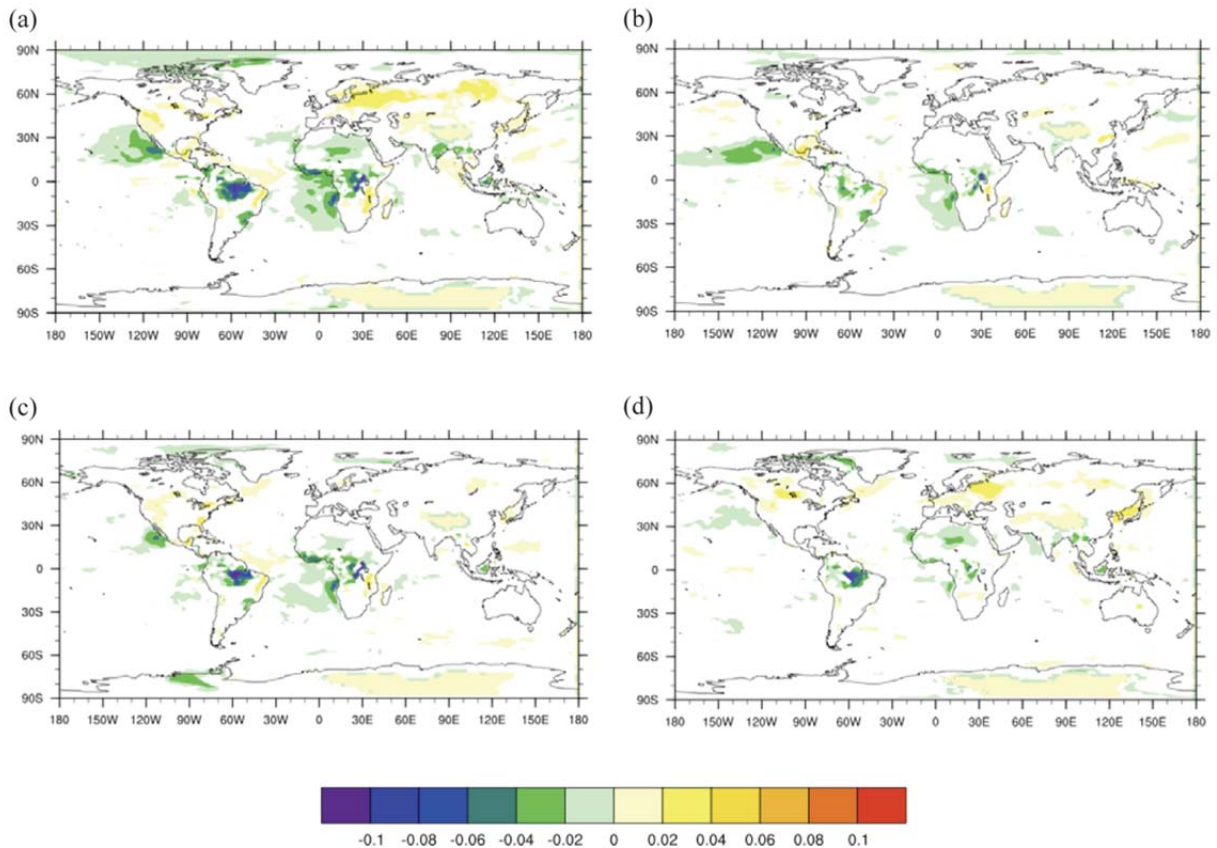


Figure 9. Low cloud cover (%): (a) Impact of just Land Cover Change (PCCR, with biofuels), (b) Impact of just Land Cover Change (OLSR, with biofuels), (c) Impact of just biofuels in PCCR case, i.e. PCCR-PCCRNb, (d) Difference between PCCR-OLSR (with biofuels). Non-shaded areas denote statistically insignificant results ($p > 0.05$).

Further, the differences seen between both the PCCR and OLSR (with biofuels) cases (Figure 10b) and the PCCR and PCCR-without-biofuels cases (Figure 10k) show that this increased surface temperature is more due to the presence of biofuels than the choice of economic scenario, in terms of the spatial extent of the areas experiencing an increase in surface temperature (i.e. the biofuel policy is responsible for large areas of warming in tropical Africa, although economic land-use policy is responsible for more of the northern hemisphere cooling).

Generally, an increase or decrease in surface net radiation leads to a concomitant increase or decrease in surface temperature, and that has been the case in the results analyzed in this study, hypothetical changes to the Bowen ratio altering surface temperature in the opposite direction to the surface net radiation notwithstanding. However, comparing the temperature differences between both the PCCR and PCCR-without-biofuels, and OLSR and OLSR-without-biofuels

cases (Figures 10a to 10d), it is apparent that the implementation of a biofuels policy has a markedly different impact on surface temperature based on the economic framework chosen.

In the PCCR economic framework (Figure 10a) the biofuel policy results in large areas of statistically significant cooling over the northern hemisphere (compared to the change in temperature due just to the change in radiative forcing (Figure 10k). The greatest decrease in temperature as a result of a biofuels policy occurs in the PCCR scenario (Figure 10a and 10e)—up to 1.75 °C over north-east Eurasia.

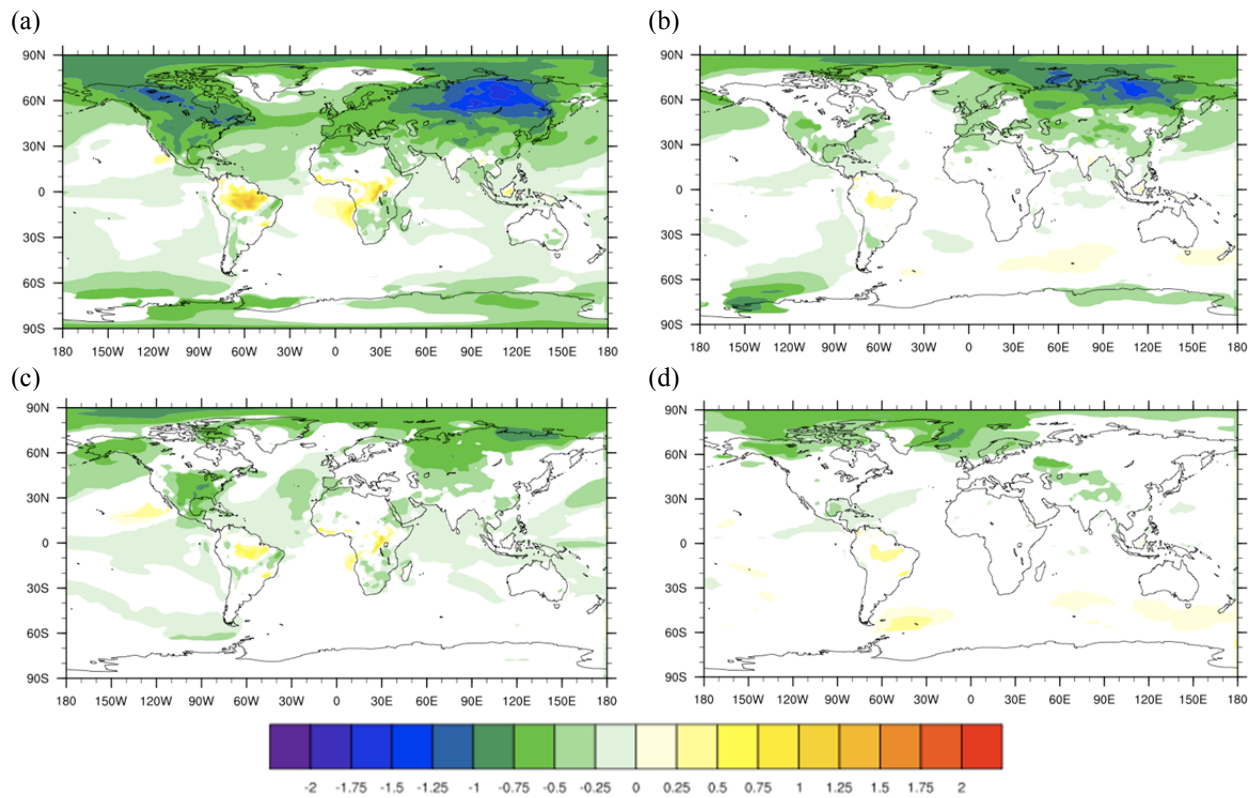


Figure 10. Changes in surface temperature (K) at reference height for all the different analyses (2050–1990) due to: (a) changing only the land cover in the PCCR scenario, with biofuels, and (b) without biofuels, (c) changing only the land cover in the OLSR scenario, with biofuels, and (d) without biofuels. Non-shaded areas denote statistically insignificant results ($p > 0.05$) (continued on page 29).

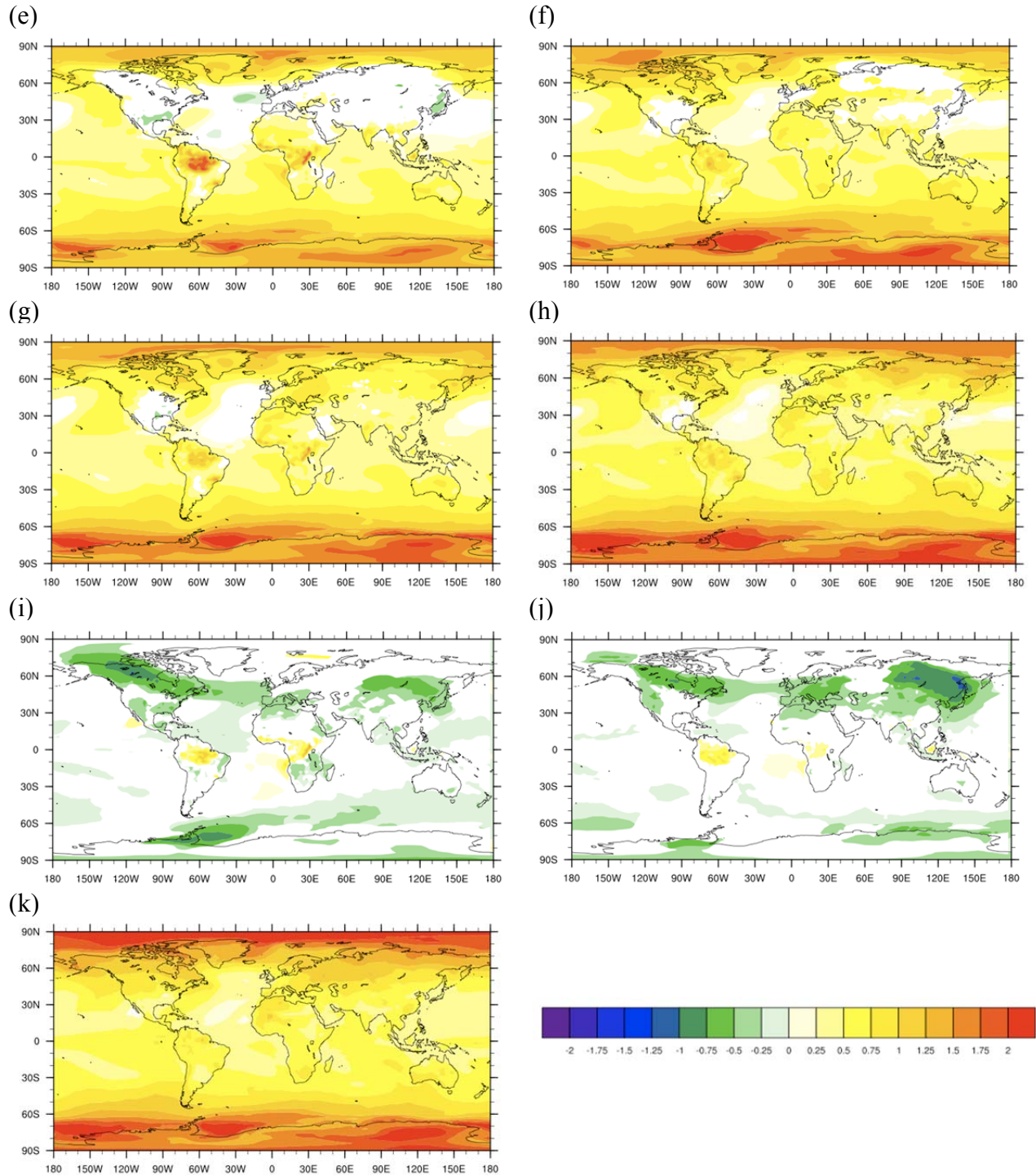


Figure 10 (cont.). Changes in surface temperature (K) at reference height for all the different analyses (2050–1990) due to the greenhouse effect plus land cover change, for the (e) PCCR scenario with biofuels, and (f) without biofuels, and (g) the greenhouse effect plus land cover change, (continued on page 30) for the OLSR scenario with biofuels, and (h) without biofuels, and (i) just the difference between the presence and absence of biofuels in the PCCR scenario (j) the difference between the two economic frameworks (PCCR-OLSR (with biofuels)), (k) just the greenhouse effect. Non-shaded areas denote statistically insignificant results ($p > 0.05$).

The biofuel policy implementation in the PCCR scenario also results in a larger extent and more severe warming in the Amazon Basin and equatorial Africa. In contrast, the implementation of a biofuels policy in the OLSR economic framework results in a smaller area of less intense statistically significant cooling in the northern and higher northern latitudes, including the majority of North America (particularly the U.S.) and central and northern Eurasia (Figure 10c).

The OLSR-with-biofuels scenario has similar albeit less pronounced patterns of warming in the tropics, except for south east Asia. This can be considered as one of the advantages of implementing the biofuel policy under the OLSR land-use scenario; the greater preservation of forested areas not only preserves biodiversity and limits carbon emissions due to deforestation (which would, in the real world, help mitigate global warming), but results in less severe and less extensive warming in the tropics due to the biophysical impacts of deforestation—preliminary precipitation results suggest that this will have a less disruptive impact on the regional hydrology of the northern South -and meso- Americas and large parts of Africa (and over land areas in general); changes in precipitation and related variables, and the causes of these changes will be explored in a following report.

Apart from the latitudinal dependency of the surface temperature results, there is also a marked seasonality in the results which also differs when considering the four different land-use/biofuels policy scenarios. As has been shown, the patterns of albedo and temperature change are strongest in the northern hemisphere, particularly in the higher latitudes, and occur to a greater extent in the PCCR scenarios. Stronger cooling also results from the implementation of a biofuel policy (both in the PCCR and OLSR frameworks, although the impact of biofuels is less severe under the OLSR land-use scenario). In North America, this cooling is particularly strong in summer (JJA) and spring (MAM) in the PCCR scenario (extending to the northern fall (SON) in the OLSR scenario), which is likely a result of decreased snow masking with deforestation in areas where it snows (leading to an increase in spring albedo), and particularly in boreal forests (Notaro *et al.*, 2008; Thomas and Rowntree, 1992). Also the greater solar angle in summer accentuates the differences in surface temperature at higher latitudes (Figure 11).

In contrast, in much of the Amazonian and African tropics, the PCCR case leads to a warming over the tropics, particularly regions where tropical forests have been replaced by biofuels. For the PCCR-biofuel scenario, this warming is greatest in June to November (JJA and SON), the tropical dry season, possibly because the regional climatic impact of deforestation accentuates this seasonal relative dryness. The tropical warming, although it occurs to a lesser extent, also shows the same seasonal dependence in the OLSR scenario.

As large and significant as the annual mean temperature changes due to LCC alone are, changes seen in the surface temperature in 2050 are primarily due to climate forcing (Figure 10k), however some buffering of the warming due to the greenhouse effect is seen, by the marked cooling from simply altering the land surface with biofuels in the PCCR scenario (Figure 10e), and to a lesser extent in the OLSR scenario (Figure 10g)). A comparison of Figures 3 and 10 shows there is generally there is a good correspondence between albedo and temperature.

It is possible to quantify which variables are the major contributors to the global mean change in surface temperature (due just to LCC) by doing a multiple linear regression analysis. For example, based on the results presented so far, the relative importance of changes in albedo and its effects on the net radiation at the surface, and the changes to the surface energy balance (i.e. the changes to the EF seen in the tropics) to the integrated temperature response, is likely to be latitude-dependent. For this analysis, the relative contribution (RC) of each independent variable in the regression analysis to the dependent variable (surface temperature) is calculated using equation (5) in Xiang and Dirmeyer (2006:1229):

$$RC_i = \alpha_i * \sigma_i \tag{4}$$

where α_i is the standard regression coefficient for a particular independent variable, and σ_i is the interannual standard deviation of that variable, calculated here using the timeseries of weighted global annual means.

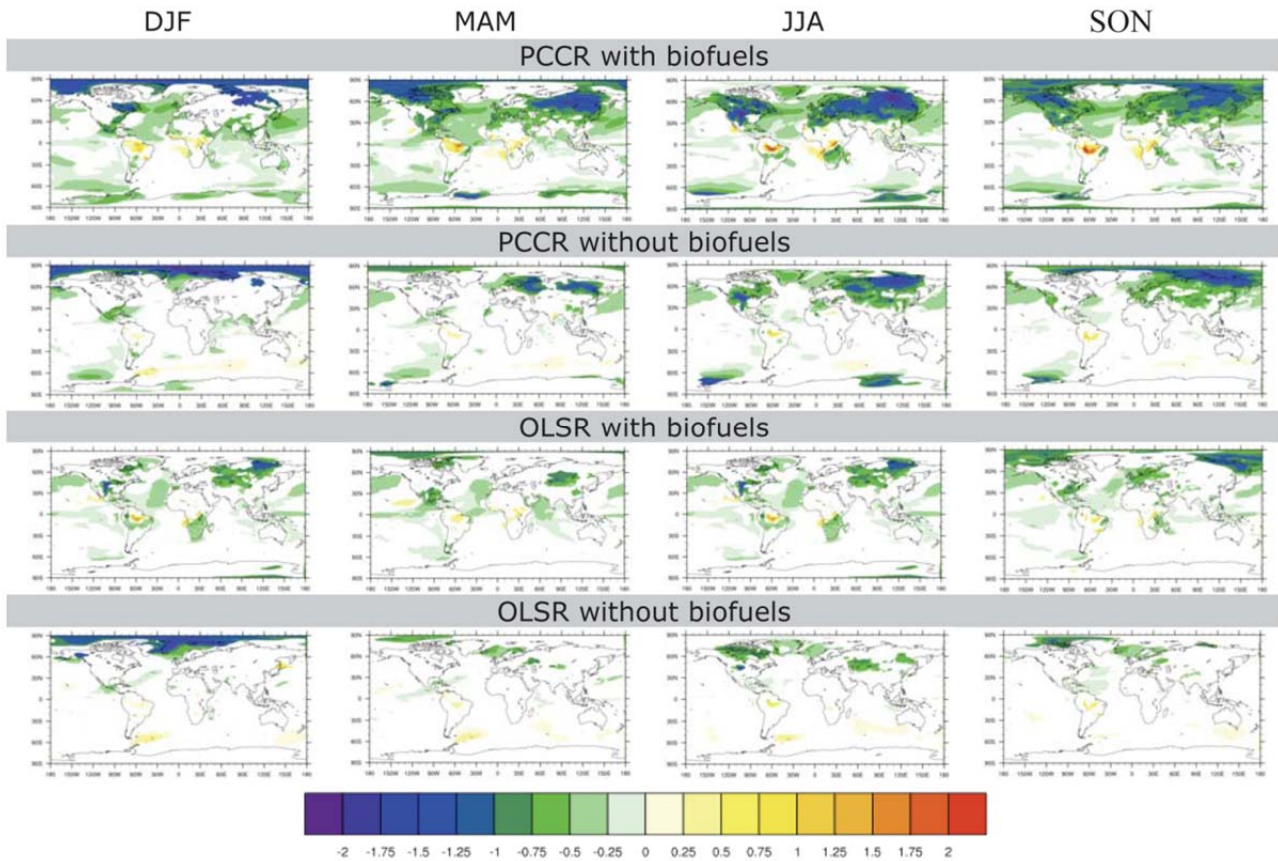


Figure 11. 2 m surface air temperature, seasonal maps: (a) DJF, (b) MAM, (c) JJA, (d) SON. Non-shaded areas denote statistically insignificant results ($p > 0.05$).

Table 6 shows that the net surface radiation is the most important variable globally and in the northern extratropics in terms of its contribution to surface temperature, but that in the tropics, LH is very much more important than anything else in determining surface temperature. These

results clearly show that the most important determinants of surface temperature are latitude-dependent, which is entirely expected—it is the net surface radiation which is the major determinant of temperature globally and in the northern extratropics, but in the tropics, the evaporative cooling over the tropical forests (or rather the change in this) is the major contributor to temperature.

The results of this analysis accord with what appears to be happening in the modeled system: the ecophysiological changes which occur with tropical deforestation, discussed above, reduce the latent heat flux over the deforested areas, causing an increase in sensible heat flux and a rise in surface air temperature.

Table 6. The Relative Contribution of Independent Variables to Surface Temperature.

RC #	Global Results		Tropical results (10°N–10°S)		Extratropical results (20–70°N)	
	PCCR	OLSR	PCCR	OLSR	PCCR	OLSR
1	Net Radiation (RC=1.44)	Net Radiation (RC=1.62)	LHF (RC=11032.5)	LHF (RC=2148.5)	Net Radiation (RC=2.40)	Net Radiation (RC=2.60)
2	LHF (RC=1.22)	PSL (RC=0.73)	Net Radiation (RC=2.85)	Net Radiation s (RC=3.07)	Net Shortwave down (RC=0.56)	LHF (RC=1.76)
3	PSL (RC=0.79)	LHF (RC=0.42)	Net shortwave flux (RC=2.54)	Net shortwave flux (RC=2.58)	LHF (RC=0.47)	Net Shortwave down (RC=0.80)
4	Net shortwave flux (RC=0.31)	Net shortwave flux (RC=0.24)	Net longwave flux (RC=2.54)	Net longwave flux (RC=0.89)	PSL (RC=0.39)	PSL (RC=0.25)
5	PBL Ht. (RC=0.13)	Net longwave flux (RC=0.12)	PBL Ht. (RC=0.08)	PSL (RC=0.27)	PBL Ht. (RC=0.12)	Net longwave flux (RC=0.23)
6	Net longwave flux (RC=0.10)	TMQ (RC=0.03)	TMQ (RC=0.07)	Net Shortwave down (RC=0.15)	Net longwave flux (RC=0.12)	PBL Ht. (RC=0.11)
7	TMQ (RC=0.03)	PBL Ht. (RC=0.02)	SST (RC=0.06)	PBL Ht. (RC=0.14)	TMQ (RC=0.05)	SHF (RC=0.02)

3.3 A Preliminary Comparison of the Biogeophysical and Biogeochemical Impacts of the Biofuel Policy

A comparison of the biogeophysical and biogeochemical impacts on surface temperature of a biofuel-based energy policy was done for the two different land-use policies used in this study (PCCR, OLSR). The biogeophysical (i.e. changes in albedo and surface turbulent fluxes due to land-use change) impact on global surface temperature (-0.119°C (S.E. = ± 0.016)) under the extensification-biofuels scenario is 1.5 times larger than the biogeochemical impact on global

temperature (i.e. CO₂ gain from biofuel production) due to biofuels, which was an increase of 0.079°C (S.E. = ± 0.012) for the PCCR-with-biofuels scenario, and of the opposite sign. The difference between the global mean 2 m air temperatures resulting from the PCCR-with-biofuels simulation which has the default CAM3.1 CO₂ concentrations and the simulation which has the carbon gain from biofuel production, is statistically significant at $\alpha= 0.05$ ($p=0.0000000976$).

The total (i.e. direct+indirect) CO₂ gain into the atmosphere for the PCCR-with-biofuels scenario is 43.9 pg C, translating to a 20.6 ppmv concentration increase, 20% of which is taken up by the terrestrial biosphere, leaving 16.55 ppmv in the atmosphere. The CO₂ gain to the atmosphere (from biofuel cropland) for the intensification scenario (3.1 pg C, translating to 1.5 ppmv (x 0.8 = 1.17 ppmv) led to a warming of 0.01°C (S.E. = ± 0.015), which was not significant at $p=0.05$). Therefore, the atmospheric CO₂ concentration at 2050 is higher than it otherwise would be in both scenarios, but only in the PCCR-with-biofuel policy scenario does this lead to a significant increase in the global temperature (**Table 7**).

Table 7. Change in 2 m surface temperature due to different factors: (i) trace-gas forcing or climate change ("CC only") from 1990–2050, (ii) the total gain of CO₂ to the atmosphere (i.e. CO₂ both directly and indirectly attributable to biofuels, for both land use scenarios, by 2050 ("CO₂ gain only"), (iii) the isolated impact of biofuels at 2050 ("Biofuels only"), (iv) land cover change for the period 1990–2050, for the four combinations of biofuel and land use scenarios ("LCC"); and three combinations of these factors. * = not statistically significant.

Factors influencing ΔT_s (policy scenario in brackets)	ΔT_s (K)
CC only	0.751
CO ₂ gain only (PCCR-with-biofuels)	0.079
CO ₂ gain only (OLSR-with-biofuels)	0.010*
Biofuels only (PCCR scenario)	-0.119
Biofuels only (OLSR scenario)	-0.098
LCC only (PCCR-with-biofuels)	-0.258
LCC only (PCCR-without-biofuels)	-0.139
LCC only (OLSR-with-biofuels)	-0.146
LCC only (OLSR-without-biofuels)	-0.048
LCC and CO ₂ gain (PCCR-with-biofuels)	-0.179
LCC and CO ₂ gain (OLSR-with-biofuels)	-0.136
CC and LCC and CO ₂ gain (PCCR-with-biofuels)	0.572
CC and LCC and CO ₂ gain (OLSR-with-biofuels)	0.615

These results show that at 2050, for the PCCR scenario, the biogeophysical impacts of a global biofuel policy (i.e. albedo and changes to the evaporative fraction) on temperature, isolated out from the impacts of land cover change over time, is a more potent and relevant

climate response, than the impact on surface temperatures of the total (i.e. direct and indirect) CO₂ gain to the atmosphere (i.e. the biogeochemical impact), but that this is not necessarily the case for the OLSR scenario (due to the lack of statistical significance). Our results extend the finding of Melillo et al. (2009b); i.e. that the carbon benefit of planting large-scale biofuel plantations is not realized by 2050 (net carbon exchange is still positive into the atmosphere), in that the atmosphere contains a residual of carbon from cleared forests. We show that this has a small impact on global surface air temperatures which is statistically significant for the PCCR land use scenario. Table 7 shows the impact on the surface temperature, over time, and at 2050, due to different, and different combinations of factors.

4. CLOSING REMARKS

Our results suggest that by the middle of this century, climate could be significantly impacted by land-use and energy policies associated with large-scale biofuel plantations. Further, we find that the change in temperature at 2050 due to the biogeophysical impact of biofuels will significantly outweigh that due to the biogeochemical impact resulting from the direct plus indirect carbon gain or loss to the atmosphere.

Generally speaking, the land-use change that led to the largest replacement of forested lands with biofuel cropland had the largest impact on temperatures around the world, and led to a regional relative cooling in most of the extratropics (with small areas of actual cooling). The replacement of rainforests in the tropics with biofuel plantations, and the subsequent disruption to the turbulent heat fluxes, lead to enhanced warming in the tropics. Thus, although the impacts of the greater deforestation from the PCCR framework occur more widely, it is the disruption to the tropical hydrology by the biofuel policy which causes more severe impacts on this region. Therefore is the case that the climate impacts associated with implementing a large scale biofuel-based energy policy depend very much on the economic land-use framework under which such a policy is implemented. Under the PCCR economic land-use framework, the growing of biofuels has more of an impact on global albedo, surface temperature, latent heat flux, sensible heat flux and net radiation, than it does under the OLSR economic pathway (particularly for albedo and temperature).

However, the PCCR framework is based on underlying econometrics which represent an extreme-for-profit-pathway. As such it should be regarded as, conceptually speaking, an upper bound (in terms of extent of deforestation) to what would likely be a more realistic economic pathway. Its consideration within this study is to demonstrate the scope of the extreme; the OLSR scenario is likely to be a more realistic outcome as it is based on empirical evidence and econometric controls that limit the rate of land-use expansion in the future. The climate impacts of the global biofuel policy are buffered in the OLSR scenario which better preserves forests by intensifying the use of existing agricultural lands.

Our study can be regarded as an exploration of the collateral climate benefit or damage of a combination of land-use and energy policies. As such, this study does not advocate any particular land-use scenario or biofuels policy. We think it is also useful to keep in mind that the large scale

deforestation scenario results in a relatively small global cooling, a cooling which is finite (as is deforestation) and which will be largely hidden by any greenhouse effect.

Also, large scale deforestation has some additional ramifications which are either not dealt with, or not dealt with explicitly, in the modeling framework used. These include, for example, the loss of the cooling effect of the cloud condensation nuclei production of boreal forests (Spracklen *et al.*, 2008), which is not modeled at all, and the impact of deforestation on permafrost which is not modeled explicitly by TEM, and which is potentially an additional positive feedback to warming (Lal *et al.*, 2000). Moreover, this study employed a generic crop parameterization of biofuels, and hence the impact of the large scale biofuel plantations on climate in these results is the same as that of the generic cropland that the version of CLM employed in this study is parameterized with. Future work will look at the impact of the biofuel policies used in this study, with a properly ecophysiologicaly-parameterized biofuel PFT.

This study is the first part of a larger one which looks at the impacts on both the localized temperature and hydroclimatological responses and the non-local circulatory patterns which arise from this; ongoing work in this area indicates that the local surface temperature response has also produced non-local precipitation and cloud responses, which indicate large scale changes in circulation patterns. Preliminary results indicate that the greater rate of deforestation and replacement by biofuels in the PCCR case has the most impact on precipitation, particularly over the land, and several non-local precipitation responses have been found, which are the result of land cover change only. These are located in the Bay of Guinea, and extending across the tropical Atlantic basin, in the ocean west of meso-America in an east-west area extending out into the middle Pacific, and in a region centered on the Arafura Sea to the north of Australia, which show an increase in precipitation.

There are some decreases in total precipitation both west and east of meso-America and in the western pacific, as well as increases in the eastern pacific (both north and south of the equator). Local precipitation responses include decreases in the Amazon basin and the interior of central and southern Africa. A preliminary analysis indicates that it is the presence of biofuels, and not the economic framework used which is largely responsible for these rainfall patterns. A regional circulation analysis will be employed in an upcoming report to comprehensively analyze these precipitation results.

Acknowledgements

This research is funded by a grant from the USA Department of Energy. The authors gratefully acknowledge the financial support for this work provided by the MIT Joint Program on the Science and Policy of Global Change through a number of Federal agencies and industrial sponsors (for the complete list see <http://globalchange.mit.edu/sponsors/current.html>).

We are grateful for the advice, expertise and insight of Andrei Sokolov¹, David Kicklighter², Jerry Melillo², Yongxia Cai¹, John Reilly¹, Angelo Gurgel³, Ben Felzer⁴ and Sergey Paltsev¹.

(1) Joint Program on the Science and Policy of Global Change, Massachusetts Institute of Technology (MIT), Cambridge, MA, USA; (2) The Ecosystems Center, Marine Biological Laboratory (MBL), 7 MBL Street, Woods Hole, MA 02543, USA; (3) Department of

Economics, University of São Paulo, Brazil; (4) Department of Earth and Environmental Sciences, Lehigh University, 31 Williams Drive, Bethlehem, PA 18015, USA.

5. REFERENCES

- Bonan, G.B., 2008: Forests and Climate Change: Forcings, Feedbacks, and the Climate Benefits of Forests. *Science*, **320**:1444–1449.
- Clarke, L.E., J.A. Edmonds, H.D. Jacoby, H.M. Pitcher, J.M. Reilly and R.G. Richels, 2007: *Scenarios of Greenhouse Gas Emissions and Atmospheric Concentrations (Sub-report 2.1A of Synthesis and Assessment Product 2.1)*. U.S. Climate Change Science Program and the Subcommittee on Global Change Research, Dept. of Energy, Office of Biological & Environmental Research: Washington, DC, USA.
- Collins, W.D., P.J. Rasch, *et al.*, 2004: *Description of the NCAR Community Atmosphere Model (CAM 3.0)*, National Center for Atmospheric Research: Boulder, Colorado, 210 pp., Technical Report NCAR/TN-464+STR.
- Farrell, A.E., R.J. Plevin, B.T. Turner, A.D. Jones, M. O’Hare and D.M. Kammen, 2006: Ethanol can contribute to energy and environmental goals. *Science*, **311**: 506–508.
- Fargione, J., J. Hill, D. Tilman, S. Polasky and P. Hawthorne, 2008: Land clearing and the biofuel carbon debt. *Science*, **319**: 1235–1238.
- Felzer, B., D. Kicklighter, J. Melillo, C. Wang, Q. Zhuang and R. Prinn, 2004: Effects of ozone on net primary production and carbon sequestration in the conterminous United States using a biogeochemistry model. *Tellus*, **56B**: 230–248.
- Gao, X., and P. Dirmeyer, 2006: A Multimodel analysis, Validation and Transferability Study of Global Soil Wetness Products, *J. Hydrometeorology*, **7**: 1218–1236.
- Gurgel, A., J. Reilly and S. Paltsev, 2007: Potential land-use implications of a global biofuels industry. *J. Agric. Food Industrial Org.* **5** (2): 1–34.
- Henderson-Sellers, A., R.E. Dickinson, T.B. Durbidge, P.J. Kennedy, K. McGuffie, and A.J. Pitman, 1993: Tropical deforestation: Modelling local to regional-scale climate change, *J. Geophys. Res.*, **98**, 7289–7315.
- Hurtt, G.C., S. Frohling, M.G. Fearon, B. Moore, E. Shevliakova, S. Malyshev, S.W. Pacala and R. A. Houghton, 2006: The underpinnings of land-use history: three centuries of global gridded land-use transitions, wood harvest activity, and resulting secondary lands. *Global Change Biol.*, **12**: 1208–1229.
- Lal, R., J.M. Kimble, and B.A. Stewart, (eds.), 2000: *Global Climate Change and Cold Regions Ecosystems*, Lewis Publishers: Boca Raton, FL, USA.
- Lee, X., M.L. Goulden, D.Y. Hollinger, A. Barr, T.A. Black, G. Bohrer, R. Bracho, B. Drake, A. Goldstein, L. Gu, G. Katul, T. Kolb, B.E. Law, H. Margolis, T. Meyers, R. Monson, W. Munger, R. Oren, U. Kyaw Tha Paw, A.D. Richardson, H.P. Schmid, R. Staebler, S. Wofsy and L. Zhao, 2011: Observed increase in local cooling effect of deforestation at higher latitude. *Nature*, **479**:384–387.
- Melillo J.M., A.C. Gurgel, D.W. Kicklighter, J.M. Reilly, T.W. Cronin, B.S. Felzer, S. Paltsev, C.A. Schlosser, A.P. Sokolov and X. Wang, 2009a: Unintended Environmental Consequences of a Global Biofuels Program, MITJPSPGC *Report 168*, January, 34 p. (http://globalchange.mit.edu/files/document/MITJPSPGC_rpt168.pdf).

- Melillo J.M., J.M. Reilly, D.W. Kicklighter, A.C. Gurgel, T.W. Cronin, S. Paltsev, B.S. Felzer, X. Wang, A.P. Sokolov, C.A. Schlosser, 2009b: Indirect Emissions from Biofuels: How Important? *Science*, **326**: 1397–1399.
- Melillo, J.M., A.D. McGuire, D.W. Kicklighter, B. Moore, C.J. Vorosmarty and A.L. Schloss 1993: Global climate change and terrestrial net primary production. *Nature*, **363**: 234–240.
- Oke T.R., 1987: *Boundary layer climates* (Second edition). Methuen. pp. 435 + xvi.
- Oleson, K.W., Y. Dai, G. Bonan, M. Bosilovich, R. Dickinson, P. Dirmeyer, F. Hoffman, P. Houser, S. Levis, G.-Y. Niu, P. Thornton, M. Vertenstein, Z.-L. Yang and X. Zeng, 2004: Technical Description of the Community Land Model (CLM), *NCAR Technical Note*, NCAR/TN-461+STR.
- Pacala, S. and R. Socolow, 2004: Stabilization wedges: solving the climate problem for the next 50 years with current technologies. *Science*, **305**: 968–972.
- Prinn, R., H. Jacoby, A. Sokolov, C. Wang, X. Xiao, Z. Yang, R. Eckhaus, P. Stone, D. Ellerman, J. Melillo, J. Fitzmaurice, D. Kicklighter, G. Holian and Y. Liu, 1999: Integrated global system model for climate policy assessment: Feedbacks and sensitivity studies. *Climatic Change*, **41**: 469–546.
- Pitman, A.J., N. de Noblet-Ducoudre, F.T. Cruz, E.L. Davin, G.B. Bonan, V. Brovkin, M. Claussen, C. Delire, L. Ganzeveld, V. Gayler, B.J.J.M. van den Hurk, P.J. Lawrence, M.K. van der Molen, C. Muller, C.H. Reick, S.I. Seneviratne, B.J. Strengers and A. Voldoire, 2009: Uncertainties in climate responses to past land cover change: First results from the LUCID intercomparison study, *Geophysical Research Letters*, **36**: L14814, doi:10.1029/2009GL039076.
- Paltsev, S., J. Reilly, H. Jacoby, R. Eckhaus, J. McFarland, M. Sarofim, M. Asadoorian and M. Babiker, 2005: The MIT Emissions Prediction and Policy Analysis (EPPA) Model: Version 4 MIT JPSPGC, Report 125, August, 72 p. (http://globalchange.mit.edu/files/document/MITJPSPGC_rpt125.pdf).
- Paltsev, S., J. Reilly, H. Jacoby, A. Gurgel, G. Metcalf, A. Sokolov and J. Holak, 2008: Assessment of US Cap-and-Trade Proposals. *Climate Policy* **8** (4): 395–420; see also MIT JPSPGC, Report 146, April, 95 p. (http://globalchange.mit.edu/files/document/MITJPSPGC_rpt146.pdf).
- Reilly, J., S. Paltsev, B. Felzer, X. Wang, D. Kicklighter, J. Melillo, R. Prinn, M. Sarofim, A. Sokolov and C. Wang, 2007: Global economic effects of changes in crops, pasture and forests due to changing climate, carbon dioxide and ozone. *Energy Policy*, **35**: 5370–5383.
- Searchinger, T., R. Heimlich, R.A. Houghton, F. Dong, A. Elobeid, J. Fabiosa, S. Tokgoz, D. Hayes and T.-H. Yu, 2008: Use of U. S. croplands for biofuels increases greenhouse gases through emissions from land-use change. *Science*, **319**: 1238–1240.
- Scharlemann, J.P.W. and W.F. Laurance, 2008: How green are biofuels? *Science* **319**: 43–44.
- Schlosser, C.A., D. Kicklighter and A. Sokolov, 2007: A Global Land System Framework for Integrated Climate-Change Assessments, MITJPSPGC Report 147, May, 60 p. (http://globalchange.mit.edu/files/document/MITJPSPGC_rpt147.pdf).
- Sokolov, A.P., C.A. Schlosser, S. Dutkiewicz, S. Paltsev, D.W. Kicklighter, H.D. Jacoby, R.G. Prinn, C.E. Forest, J.M. Reilly, C. Wang, B. Felzer, M.C. Sarofim, J. Scott, P.H. Stone, J.M. Melillo and J. Cohen, 2005: The MIT Integrated Global System Model (IGSM) Version 2: Model Description and Baseline Evaluation, MITJPSPGC Report 124, July, 40 p. (http://globalchange.mit.edu/files/document/MITJPSPGC_rpt124.pdf).

- Sokolov, A. P., D. W. Kicklighter, J. M. Melillo, B. S. Felzer, C. A. Schlosser and T. W. Cronin, 2008: Consequences of considering carbon-nitrogen interactions on the feedbacks between climate and the terrestrial carbon cycle. *Journal of Climate*, **21**: 3776–3796.
- Spracklen, D.V., B. Bonn, and K.S. Carslaw, 2008: Boreal forests, aerosols and the impacts on clouds and climate. *Phil. Trans. R. Soc. A*, doi:10.1098/rsta.2008.0201. Published online. 13 pp.
- The Royal Society, 2008: Sustainable Biofuels: Prospects and Challenges. Science Policy Section, The Royal Society: London (<http://royalsociety.org/document.asp?id=7366>).
- Tilman, D., J. Hill and C. Lehman, 2006: Carbon-negative biofuels from low-input high-diversity grassland biomass. *Science* **314**: 1598–1600.
- Vertenstein, M., T. Craig, T. Henderson, S. Murphy, G.R. Carr Jr. and N. Norton, 2004: CCSM3.0 User's Guide. NCAR.
- Wang, C., and R. G. Prinn, 2010: Potential climatic impacts and reliability of very large-scale wind farms, *Atmos. Chem. Phys.* **10**, 2053–2061.
- Xiang, G., and P.A. Dirmeyer, 2006: A multimodel analysis, validation, and transferability study of global soil wetness products. *Journal of Hydrometeorology*, **7**:1218–1236.

APPENDIX

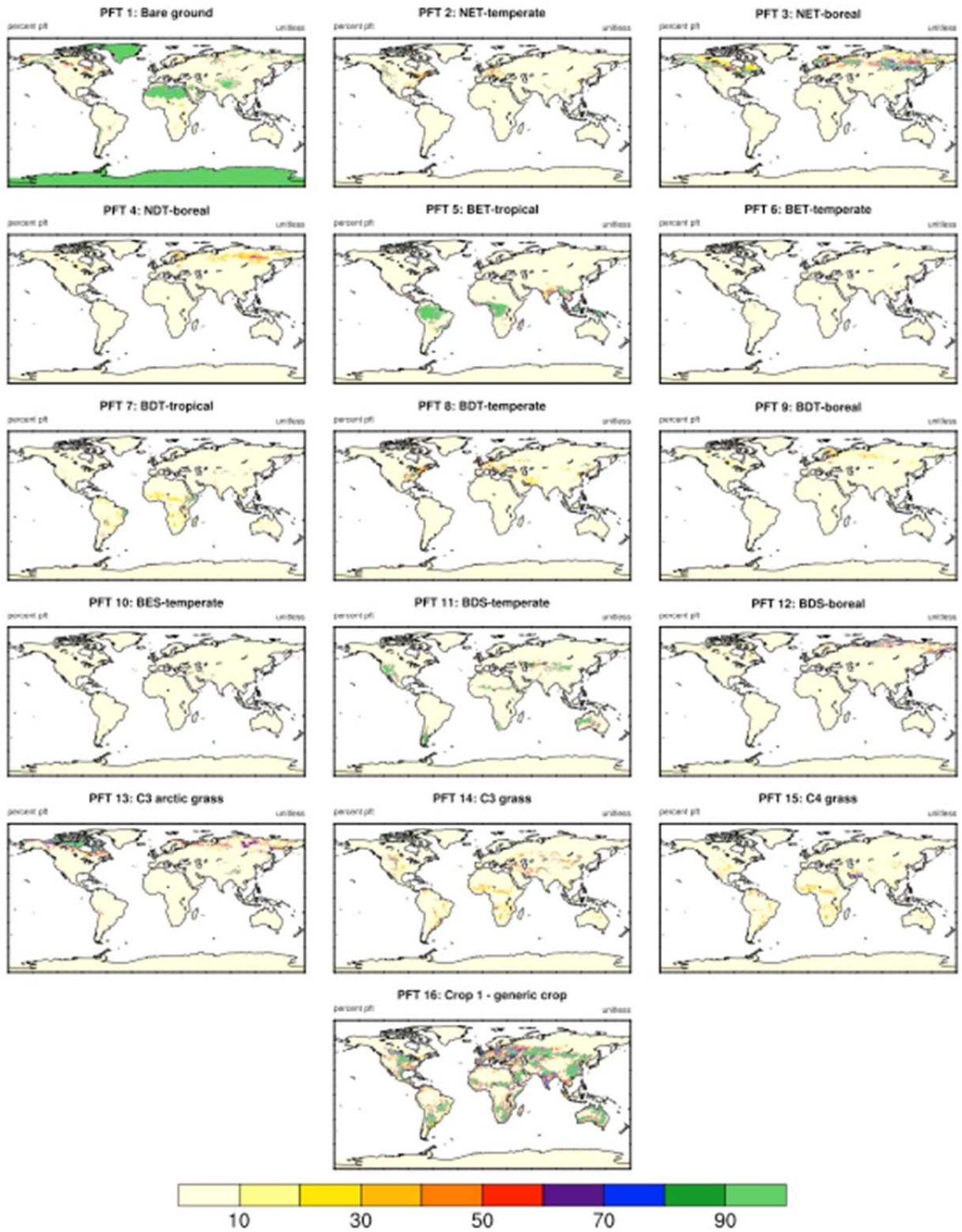


Figure A1 (a). Maps showing the percent coverage of each of the 16 Plant Functional Types (PFTs) present in 1990, prior to the implementation of any land-use or biofuel-based energy policies.

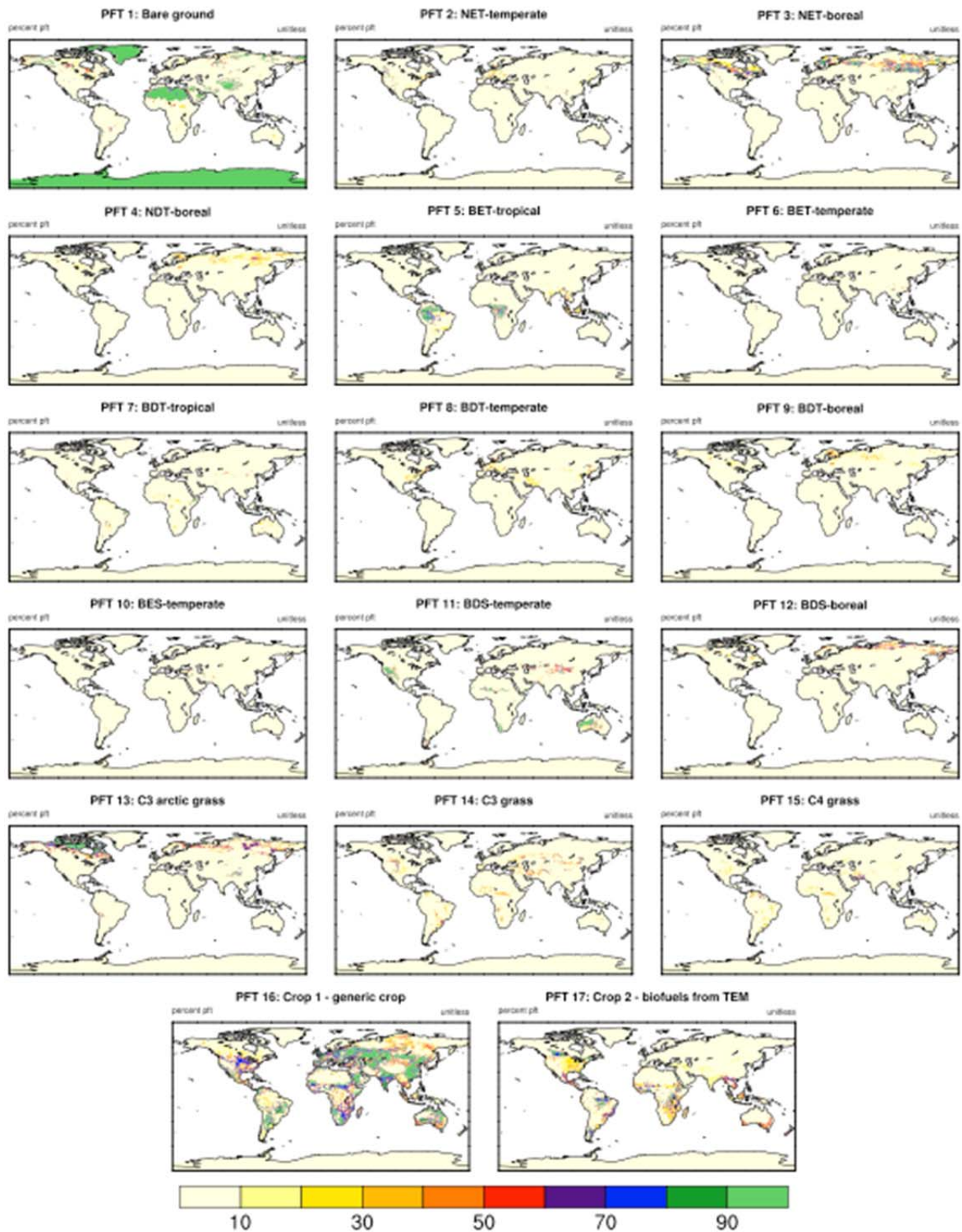


Figure A1 (b). Maps showing the percent coverage of each of the 17 Plant Functional Types (PFTs) present in 2050 in the PCCR-with-biofuels scenario.

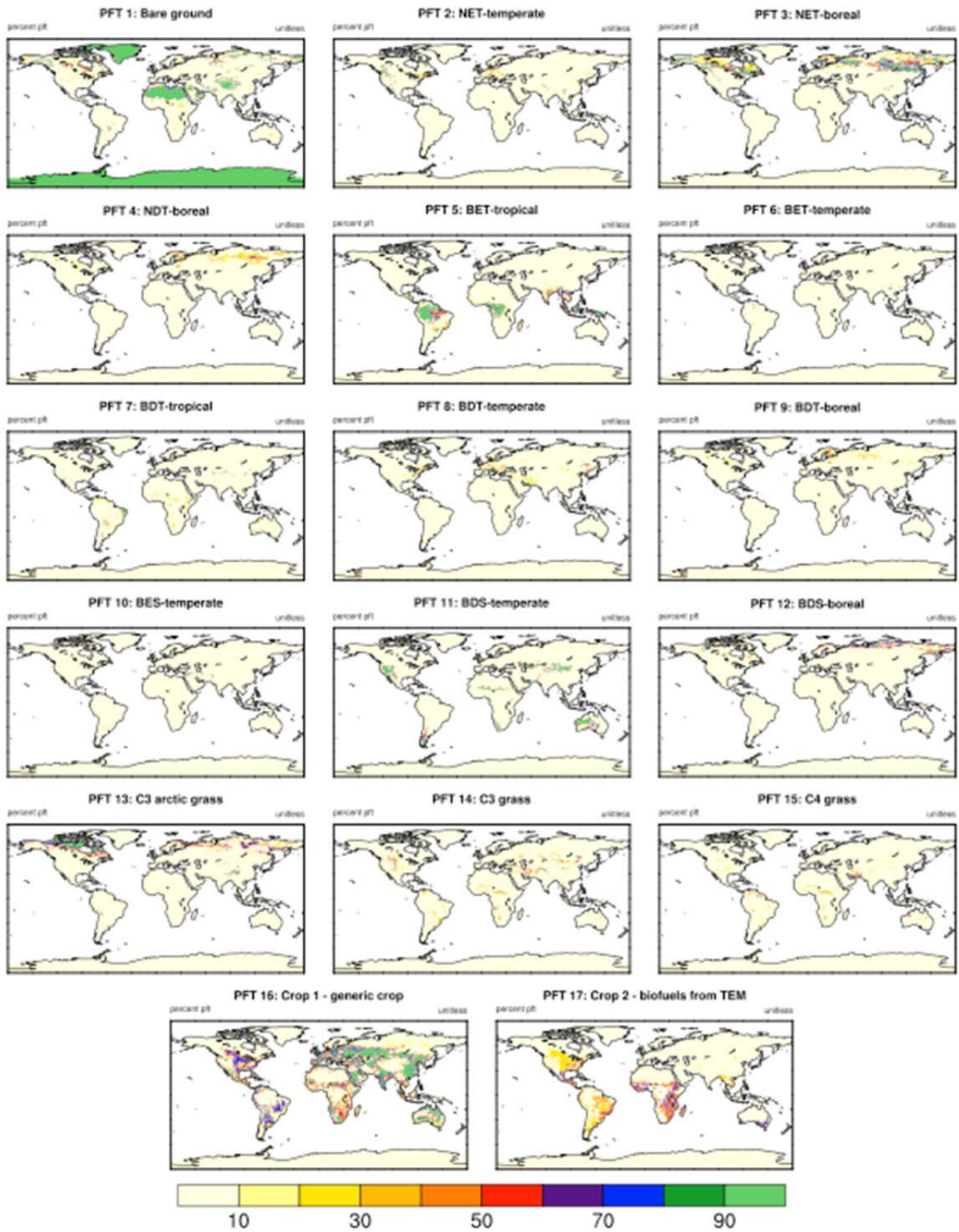


Figure A1 (c). Maps showing the percent coverage of each of the 17 Plant Functional Types (PFTs) present in 2050 in the OLSR-with-biofuels scenario.

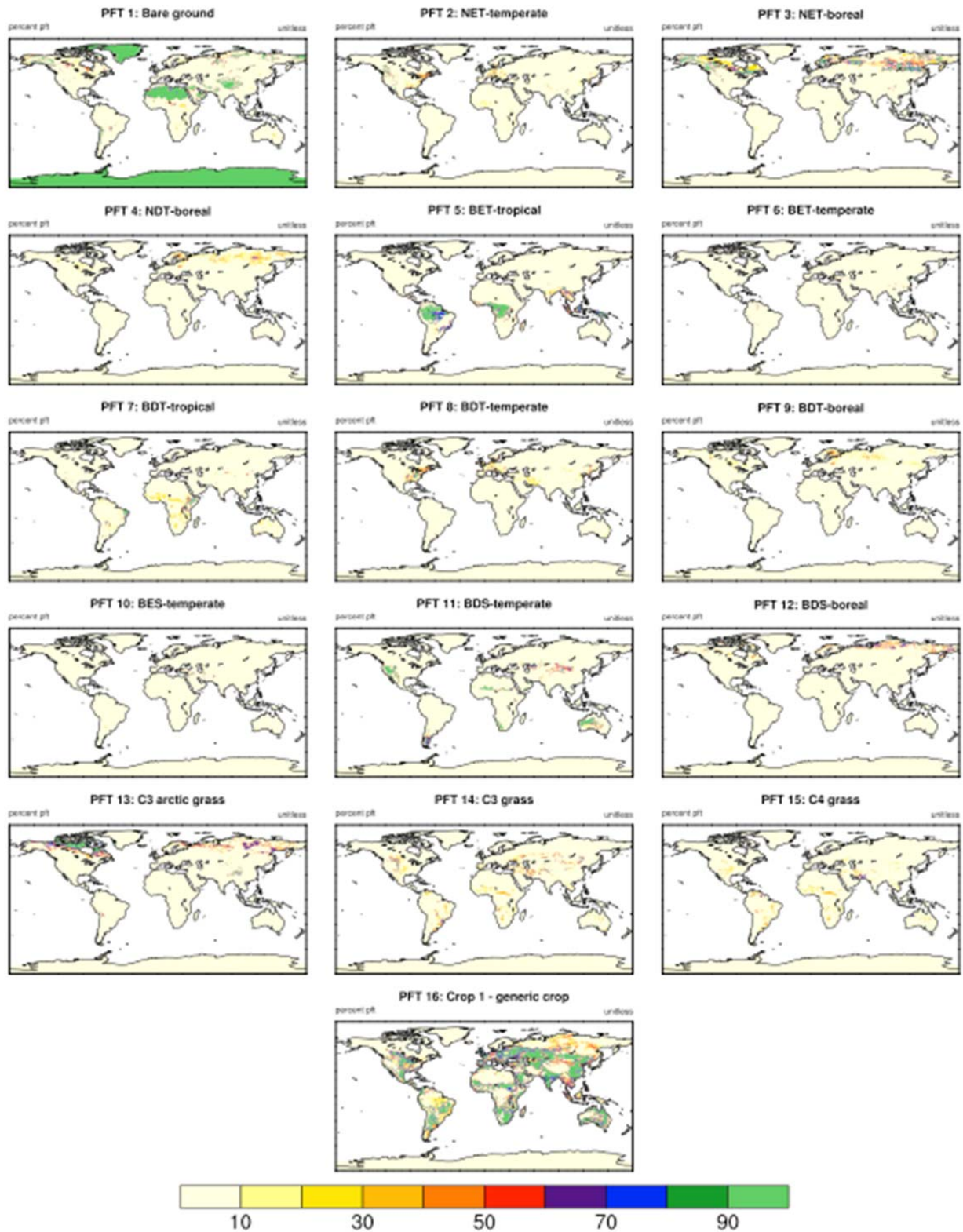


Figure A1 (d). Maps showing the percent coverage of each of the 16 Plant Functional Types (PFTs) present in 2050 in the PCCR-without-biofuels scenario.

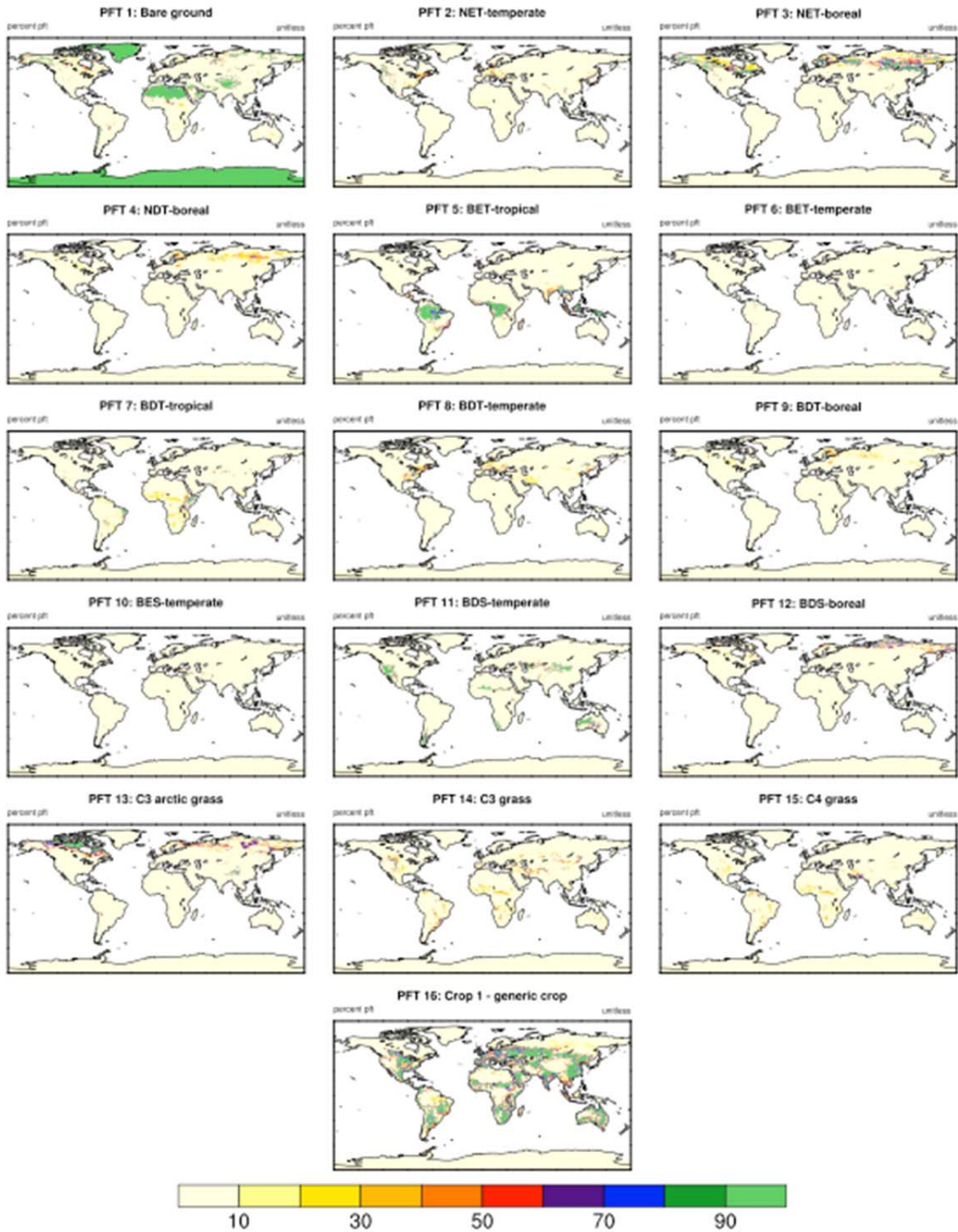


Figure A1 (e). Maps showing the percent coverage of each of the 16 Plant Functional Types (PFTs) present in 2050 in the OLSR-without-biofuels scenario.

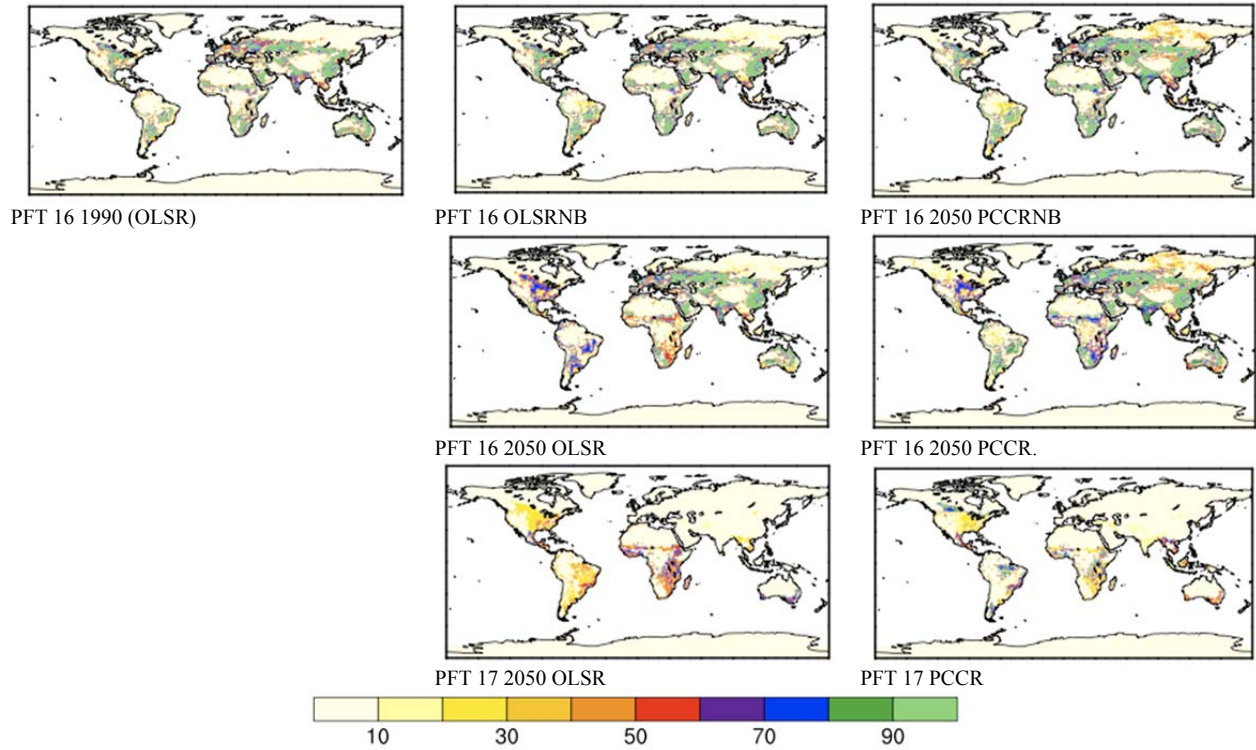


Figure A2. The effect on cropland in 2050 of the introduction of biofuel crops in 2026. No economic scenarios were implemented before 2000. PFT 16 is the CLM generic cropland, and PFT 17 represents the biofuels in both the PCCR and OLSR scenarios.

REPORT SERIES of the MIT Joint Program on the Science and Policy of Global Change

FOR THE COMPLETE LIST OF JOINT PROGRAM REPORTS:
<http://globalchange.mit.edu/pubs/all-reports.php>

184. **Will Border Carbon Adjustments Work?** *Winchester et al.* February 2010
185. **Distributional Implications of Alternative U.S. Greenhouse Gas Control Measures** *Rausch et al.* June 2010
186. **The Future of U.S. Natural Gas Production, Use, and Trade** *Paltsev et al.* June 2010
187. **Combining a Renewable Portfolio Standard with a Cap-and-Trade Policy: A General Equilibrium Analysis** *Morris et al.* July 2010
188. **On the Correlation between Forcing and Climate Sensitivity** *Sokolov* August 2010
189. **Modeling the Global Water Resource System in an Integrated Assessment Modeling Framework: IGSM-WRS** *Strzepek et al.* September 2010
190. **Climatology and Trends in the Forcing of the Stratospheric Zonal-Mean Flow** *Monier and Weare* January 2011
191. **Climatology and Trends in the Forcing of the Stratospheric Ozone Transport** *Monier and Weare* January 2011
192. **The Impact of Border Carbon Adjustments under Alternative Producer Responses** *Winchester* February 2011
193. **What to Expect from Sectoral Trading: A U.S.-China Example** *Gavard et al.* February 2011
194. **General Equilibrium, Electricity Generation Technologies and the Cost of Carbon** *Abatement Lanz and Rausch* February 2011
195. **A Method for Calculating Reference Evapotranspiration on Daily Time Scales** *Farmer et al.* February 2011
196. **Health Damages from Air Pollution in China** *Matus et al.* March 2011
197. **The Prospects for Coal-to-Liquid Conversion: A General Equilibrium Analysis** *Chen et al.* May 2011
198. **The Impact of Climate Policy on U.S. Aviation** *Winchester et al.* May 2011
199. **Future Yield Growth: What Evidence from Historical Data** *Gitiaux et al.* May 2011
200. **A Strategy for a Global Observing System for Verification of National Greenhouse Gas Emissions** *Prinn et al.* June 2011
201. **Russia's Natural Gas Export Potential up to 2050** *Paltsev* July 2011
202. **Distributional Impacts of Carbon Pricing: A General Equilibrium Approach with Micro-Data for Households** *Rausch et al.* July 2011
203. **Global Aerosol Health Impacts: Quantifying Uncertainties** *Selin et al.* August 2011
204. **Implementation of a Cloud Radiative Adjustment Method to Change the Climate Sensitivity of CAM3** *Sokolov and Monier* September 2011
205. **Quantifying the Likelihood of Regional Climate Change: A Hybridized Approach** *Schlosser et al.* October 2011
206. **Process Modeling of Global Soil Nitrous Oxide Emissions** *Saikawa et al.* October 2011
207. **The Influence of Shale Gas on U.S. Energy and Environmental Policy** *Jacoby et al.* November 2011
208. **Influence of Air Quality Model Resolution on Uncertainty Associated with Health Impacts** *Thompson and Selin* December 2011
209. **Characterization of Wind Power Resource in the United States and its Intermittency** *Gunturu and Schlosser* December 2011
210. **Potential Direct and Indirect Effects of Global Cellulosic Biofuel Production on Greenhouse Gas Fluxes from Future Land-use Change** *Kicklighter et al.* March 2012
211. **Emissions Pricing to Stabilize Global Climate** *Bosetti et al.* March 2012
212. **Effects of Nitrogen Limitation on Hydrological Processes in CLM4-CN** *Lee & Felzer* March 2012
213. **City-Size Distribution as a Function of Socio-economic Conditions: An Eclectic Approach to Down-scaling Global Population** *Nam & Reilly* March 2012
214. **CLiCrop: a Crop Water-Stress and Irrigation Demand Model for an Integrated Global Assessment Modeling Approach** *Fant et al.* April 2012
215. **The Role of China in Mitigating Climate Change** *Paltsev et al.* April 2012
216. **Applying Engineering and Fleet Detail to Represent Passenger Vehicle Transport in a Computable General Equilibrium Model** *Karplus et al.* April 2012
217. **Combining a New Vehicle Fuel Economy Standard with a Cap-and-Trade Policy: Energy and Economic Impact in the United States** *Karplus et al.* April 2012
218. **Permafrost, Lakes, and Climate-Warming Methane Feedback: What is the Worst We Can Expect?** *Gao et al.* May 2012
219. **Valuing Climate Impacts in Integrated Assessment Models: The MIT IGSM** *Reilly et al.* May 2012
220. **Leakage from Sub-national Climate Initiatives: The Case of California** *Caron et al.* May 2012
221. **Green Growth and the Efficient Use of Natural Resources** *Reilly* June 2012
222. **Modeling Water Withdrawal and Consumption for Electricity Generation in the United States** *Strzepek et al.* June 2012
223. **An Integrated Assessment Framework for Uncertainty Studies in Global and Regional Climate Change: The MIT IGSM** *Monier et al.* June 2012
224. **Cap-and-Trade Climate Policies with Price-Regulated Industries: How Costly are Free Allowances?** *Lanz and Rausch* July 2012.
225. **Distributional and Efficiency Impacts of Clean and Renewable Energy Standards for Electricity** *Rausch and Mowers* July 2012.
226. **The Economic, Energy, and GHG Emissions Impacts of Proposed 2017–2025 Vehicle Fuel Economy Standards in the United States** *Karplus and Paltsev* July 2012
227. **Impacts of Land-Use and Biofuels Policy on Climate: Temperature and Localized Impacts** *Hallgren et al.* August 2012